



Structural uncertainty in the direct human forcing of future global burned area

Oliver Perkins^{1,2}, Olivia Haas^{1,3}, Matthew Kasoar^{1,4}, Apostolos Voulgarakis^{1,4,5}, and James D. A. Millington^{1,2}

¹The Leverhulme Centre for Wildfires, Environment, and Society, Imperial College London, London, UK.

²Department of Geography, King's College London, London, UK.

³Geography and Environmental Science, University of Reading, Reading, UK.

⁴Department of Physics, Imperial College London, London, UK.

⁵School of Chemical and Environmental Engineering, Technical University of Crete, Kounoupidiana, Greece.

Correspondence to: Oliver Perkins (oliver.perkins@kcl.ac.uk)

Abstract. The first fire model intercomparison project (FIREMIP) gave rise to two distinct proposals around how best to improve the fire modules of dynamic global vegetation models. The first proposal was to develop representation of direct human impacts on burned area, particularly managed fire use in agriculture and other land management. The second proposal was to improve representation of the ecological dimensions of fire, including relationships of fuel load, connectivity, dryness and fire. Here, we present future projections from two models that have attempted to advance model representation and understanding of the human (WHAM-INFERNO) and ecological (Haas) dimensions of global fire regimes. The models project radically different future burned area for the same sets of scenario forcings. There is particularly strong disagreement regarding direct human impacts (or “direct human forcing”) of global burned area: differences in model assessment of the impact of direct human forcing is greater between models than between scenarios. We show how such structural uncertainty constrains understanding of climate change adaptation, including its limits and pitfalls. Differences in model outputs are largely traceable back to model assumptions. Hence, we argue that advances made by the two models could be combined in a future fire model that better captures the socio-economic and ecological drivers of burned area. We identify key challenges to the development of such integrated socio-ecological models, highlighting crucial uncertainties around how anthropogenic and biophysical factors interact to produce patterns of fuel fragmentation and hence fire spread. Overall, advancing understanding of the interactions between human and biophysical drivers of fire remains a central challenge in fire science.



30 1 Introduction

Fire is simultaneously a fundamental Earth-system process (Jones et al., 2022) and central to many lives and livelihoods globally (Smith et al., 2022). These two dimensions are well demonstrated by diverging trends in satellite observations: in the boreal North, burned area, fire intensity and emissions are increasing due to climate change (Cunningham et al., 2024; Jones et al., 2024), but total global burned area is declining, primarily due to land use change in the tropics (Andela et al., 35 2017; Chen et al., 2023). Similarly, observational and model studies both increasingly point to a contrast between anthropogenic land management fires (hereafter “managed fires”), which are smaller, less intense and have lower interannual variability (IAV; Randerson et al., 2012; Archibald et al., 2013; Shuman et al., 2022) than unmanaged wildfires that are generally larger and more intense (hereafter ‘wildfires’; Kirchmeier-Young et al., 2024; McClure et al., 2024). Furthermore, managed fires are likely declining globally owing to increased land use intensity (Perkins et al., 2024a; Smith et al., 2022), 40 whilst trends in wildfires are more strongly influenced by climate change, and hence have higher IAV (Burton et al., 2024; Gincheva et al., 2024).

A primary tool available to understand the complex drivers of present-day fire regimes are global models, typically dynamic global vegetation models (DGVMs; Rabin et al., 2017). These are the land surface components of Earth system models used to project the response of the climate to anthropogenic greenhouse gas emissions (Kasoar et al., 2024). DGVMs 45 have struggled to capture the land-use-driven decline in burned area and instead often show increasing historical burned area in line with climate forcings (Teckentrup et al., 2019). However, at the same time, DGVMs have also struggled to capture the climate-driven interannual variability of fire (Hantson et al., 2020).

Consequently, the first fire model intercomparison project (FIREMIP; Rabin et al., 2017) gave rise to two distinct proposals concerning how best to improve the performance of global-scale fire models. The first proposal was that models 50 needed to improve the representation of direct human impacts on fire regimes (Ford et al., 2021). Such direct human impacts (or ‘direct human forcings’; hereafter ‘DHF’) include intentional human fire use in agriculture and landscape management (Forrest et al., 2024; Millington et al., 2022), fire suppression (Kreider et al., 2024), and the spillover effects of land use changes including cropland conversion and road building (Bowring et al., 2024; Rosan et al., 2022). The proposal to focus on improving representation of DHF was driven by the finding that models had no agreement on how DHF had influenced 55 burned area over the last century, with estimates ranging from c. 50% increase to c. 50% decrease in burned area from 1900 levels (Teckentrup et al., 2019). Such inter-model disagreement was underpinned by highly simplistic representations of humans in the existing global fire models, often restricted simply to a function of population density (Kasoar et al., 2024). The second proposal was to focus on improving representation of the ecological dimensions of fire regimes, including the role of fuel loads and fire-specific adaptations in vegetation (Harrison et al., 2021). This suggestion was given weight by the 60 fact that models which better captured the global distribution of gross primary production (GPP) also better captured the distribution of burned area (Hantson et al., 2020).



Here, we compare projections from two global fire models, one that attempts to improve representation of the socio-economic dimensions of fire and the other to improve the ecological. We assess the degree to which differences in assumptions about direct human drivers of burned area influence future fire regimes simulated by these models. The first model is WHAM-INFERNO: the offline integration of a global agent-based model of human fire use and management (WHAM!; Perkins et al., 2024a) with the JULES-INFERNO dynamic global vegetation model (Mangeon et al., 2016). WHAM-INFERNO is the first coupled model ensemble to explicitly represent (and distinguish between) managed human fire uses – spanning agricultural burning, fire use in hunting and gathering, and prescribed fire use – and their interactions with fire’s biophysical drivers (Perkins et al., 2025a). The second model is the generalised linear model of Haas et al., (2022; hereafter “Haas model”), which focused on gross primary production as the underlying driver of global fire regimes, and in its original publication is driven by outputs from the process-based P-model of photosynthesis (Stocker et al., 2020; Wang et al., 2017).

Both models are better able to reproduce the observed spatial distribution of burned area than models that participated in the latest published FireMIP assessments (WHAM: $r = 0.83$, Haas: $r = 0.84$, FIREMIP: $0.50 < r \leq 0.81$; Teckentrup et al., 2019). Yet, the two models have profoundly different structures and assumptions, particularly regarding the role of humans (Table 1). WHAM! conceptualises humans as active participants in fire regimes – making decisions about where, when and how much to burn according to boundedly rational land use objectives (Perkins et al., 2022). Humans respond both to socio-economic conditions, for example their access to fire-free land management methods (e.g. mechanisation, chemical fertilisers), and environmental conditions, for example the net primary production of a cattle pasture (Perkins et al., 2024a). However, anthropogenic management of fire regimes is far from perfect, and at least 50% of burned area is generated by uncontrolled wildfires (Perkins et al., 2025a). These are either ignited by lightning, accidental or incidental anthropogenic fires, or are ‘escaped fires’: fires that were ignited intentionally for a specific purpose but which subsequently grew out of control (Cano-Crespo et al., 2015; Li et al., 2025). WHAM! projects the burned area from successfully controlled human fires, whilst JULES-INFERNO calculates the burned area of free-burning wildfires based on biophysical factors.

By contrast, in the Haas model the effect of human activity is represented primarily via landscape fragmentation through road building and cropland conversion (Haas et al., 2022). As such, the largest human influence on fire is indirect, through land cover changes which perturb underlying ecological processes, rather than direct (intentional) interaction with the fire regime. The model adopts an empirically-defined, weakly positive relationship between human population density and burned area, but implicitly it is assumed that many ecosystems are “ignition saturated”: the presence of anthropogenic fire use does not necessarily lead to increased overall burned area but rather serves primarily to reduce individual fire size proportionally to the number of additional fires (Archibald et al., 2012; Knorr et al., 2014). Both models, then, seek to move away from the representation of humans primarily as generators of ‘ignitions’, yet they do this in opposite ways. The Haas model focuses on fuel connectivity, whilst WHAM-INFERNO highlights human impacts not only on fire ignition, but also on controlling fire spread (Kasoar et al., 2024).



Table 1: Representation of differing dimensions of global fire regimes in the WHAM-INFERNO ensemble (Perkins et al., 2025a) and the Haas generalised linear model (Haas et al., 2022).

Model process	Model representation	
	WHAM-INFERNO	Haas model
Climate	INFERNO combines process-based & empirical representation of climate impacts on fire in a vegetation flammability calculation. An upper limit is derived from the vapour pressure deficit, which is then constrained by fuel availability, precipitation, and soil and atmospheric moisture content.	Empirically defined as a function of the vapour pressure deficit, dry days and their seasonality, diurnal temperature range, and the interaction of windspeed and temperature (maximum wind speed of the hottest month).
Vegetation	13 plant functional types are each assigned an empirical mean fire size.	Gross primary production (GPP) and its seasonality are the fundamental model drivers. In its original conceptualisation, these were sourced from the P-model to ensure faithful representation (Stocker et al., 2020). Relationships of GPP to burned area in the model are empirical.
Human fire use	Represented in detail as a function of land system and land user types and their relationship with varying socio-ecological contexts.	Not represented beyond a weakly positive empirical relationship between population density and burned area.
Human fire management	Fire control – the degree to which managed fires stay managed and fire suppression intensity (i.e. fire-fighting) are both represented explicitly.	Not represented
Landscape fragmentation	Road density and cropland cover decrease the mean fire size, and hence burned area, of unmanaged wildfires. However, cropland can also increase managed burned area where agricultural residue burning occurs.	Represented through cropland conversion and roads; these empirically reduce the burned area of all fires.



This paper presents and analyses model outputs from WHAM-INFERNO and the Haas model. It explores how the two models' distinctly different conceptualisations of the DHF of burned area shape model projections under climate and socio-economic change. We assess whether there are commonalities between models, despite their contrasting assumptions and structures. Discussion focuses on the distinct fire-adaptation challenges under different Shared Socio-economic Pathways and the key priorities for future research highlighted by the model intercomparison.

2 Methods

We present outputs from model runs of WHAM-INFERNO and the Haas model for two Shared Socio-economic Pathways (SSPs) used in the Intersectoral Model Intercomparison Project (ISIMIP; Lange, 2019). These are SSP1 with representative concentration pathway 2.6 (SSP1-2.6) and SSP3 with representative concentration pathway 7.0 (SSP3-7.0). We adopt these as they represent a range of warming scenarios from low (SSP1-2.6) to high (SSP3-7.0). We first briefly introduce WHAM-INFERNO and the Haas model, as well as describing their respective forcing data sets (Table 2). We then describe bias correction and harmonisation procedures for forcing data to be used with both models. Finally, we describe experiments undertaken and analysis of model outputs. All code and data to reproduce results presented here are made available as Perkins et al., (2025b).

2.1 Model description & setup

2.1.1 WHAM-INFERNO

WHAM-INFERNO combines runs of the WHAM! global model of human fire and management with the JULES-INFERNO dynamic global vegetation model. WHAM! was setup as described in Perkins et al., (2024a). The offline model coupling with JULES-INFERNO is described in detail in Perkins et al., (2025a). Hence, here we provide a brief overview of model structure, before describing the calculation of vegetation flammability for future model runs.

WHAM-INFERNO calculates burned area as the sum of managed and unmanaged fire. Managed fire is calculated by WHAM!, whilst unmanaged fire is calculated by INFERNO. The six managed fire use types in WHAM! are those originally identified in Millington et al., (2022): crop field preparation (i.e. shifting cultivation), crop residue burning, hunting and gathering, pasture management, pyrome management (the use of fire explicitly to reduce the intensity of the fire regime by fragmenting fuel loads), and vegetation clearance (deforestation). Indigenous fire use frequently does not sit neatly in any one purpose: fires may be lit for multiple purposes at the same time (Nikolakis and Roberts, 2020). Hence “hunter gatherer” fire use in WHAM! attempts to capture the overall systems of fire use practiced by such communities (Christianson et al., 2022). WHAM! calculates managed fire use through the modelled distribution of “agent functional types” (AFTs; Arneth et al., 2014), which aim to capture characteristic syndromes of human fire use and management across different land use systems - arable farming, livestock farming, forestry and non-extractive land uses (Perkins et al., 2022; Table S1).



Unmanaged burned area is calculated by INFERNO as:

130 $Burned_area_{UM} = Fires_{UM} * Flammability_{pft} * \overline{BA}_{pft}$ (1)

where $Burned_area_{UM}$ is the burned area from unmanaged fires, \overline{BA}_{pft} is a mean fire size per plant functional type, and $Fires_{UM}$ is the sum of lightning fires, escaped managed fires, arson, and a constant rate of accidental / miscellaneous fires. WHAM! calculates a probability of fire escape for each agent functional type and managed fire use type, as well as numbers of fires due to arson – defined as fire use explicitly as a weapon (Perkins et al., 2024a). Lightning strikes and the background rate of incidental fires are reduced linearly with WHAM!’s calculation of fire suppression intensity.

135

INFERNO’s flammability calculation (eq. 2) serves the role of capturing the impact of climate, hydrology, and fuel availability on fire (Mangeon et al., 2016; Table 1). This was reproduced offline such that all the inputs to the flammability calculation could be bias corrected to allow comparison with Haas-model outputs (see section 2.2). As in Mangeon et al., (2016), INFERNO calculates flammability as:

140 $Flammability_{pft} = VP * f(RH) * f(Fuel_{pft}) * f(\theta) * f(Precip)$ (2)

where VP is the saturation vapour pressure, $f(RH)$ is a function of relative humidity, $f(Fuel_{pft})$ is a function of fuel availability, $f(\theta)$ is a function of soil moisture content, and $f(Precip)$ a function of precipitation. In other words, the (temperature dependent) saturation vapour pressure sets an upper ceiling on flammability, which is then reduced by four (0-1) constraint functions. Datasets used for this offline calculation were sourced from JULES’ ISIMIP3b outputs (detailed in Table 2).

145

Finally, the coupling of WHAM! with JULES-INFERNO was conducted as in Perkins et al., (2025a); the calibration described therein identified 10 pareto optimal combinations of model free parameters. These free parameters include the mean burned area per fire for each plant functional type in INFERNO (as in eq. 1), the impact of road density in reducing this burned area per fire, and parameters to calibrate the impact of fire suppression (see Perkins et al., 2025a, supplementary information for details). We ran the WHAM-INFERNO coupled model using each of these parameter sets and present the full-range of outputs for WHAM-INFERNO runs. When comparing with the Haas model, we take the mean of these runs as the maximum likelihood (best) estimate.

150

2.1.2 Haas generalised linear model

The Haas model was developed to capture overall spatial patterns of burnt area given background climate and vegetation state. It was applied as originally presented in Haas et al., (2022), with three changes. Firstly, the model was run at the same resolution as WHAM-INFERNO (1.875° x 1.25°). Secondly, the Haas model was originally trained against GFED4 burned area (Giglio et al., 2013; Haas et al., 2022). However, as the 5th edition of GFED has revealed burned area to be as much as 61% higher than previously estimated (Chen et al., 2023), and WHAM-INFERNO adopts GFED5 as its baseline, the Haas model was retrained against this more recent dataset. Thirdly, rather than using the P-model gross primary production (GPP),

155



the MUSES satellite-derived product was used (Wang et al., 2021). This was to ensure comparability with WHAM!, which uses MUSES NPP data as a baseline input (Table 2).

2.2 Bias correction of scenario forcing

Our goal was to run both WHAM-INFERNO and the Haas with initial states and forcings as similar as possible, such that outputs were directly comparable. Therefore, we sought to bias correct scenario forcings to a common baseline state. We sourced future biophysical forcing data from the Intersectoral Model Intercomparison Project 3b (Frieler et al., 2017), using runs forced by the UK Earth System Model (Sellar et al., 2020). For each variable, we identified a reference dataset for the present day (Table 2) and took 2020 as a common baseline. We then calculated the annual anomaly of the scenario forcing (compared to 2020 in the scenario data) and added this to the baseline reference state. For variables without readily available remote sensing observations - leaf and soil carbon content and soil moisture - we adopted JULES ISIMIP3a outputs using ERA5 forcings (Frieler et al., 2024) as the reference. For soil moisture, INFERNO uses the top-layer of soil as represented by JULES only and hence has no direct observational analogue (Mangeon et al., 20216).

The main challenge for model input data harmonisation was in the models' respective treatment of land covers. Both WHAM-INFERNO and the Haas model treat cropland as an explicitly anthropogenic land use category. However, WHAM-INFERNO treats pasture as a separate land cover class from natural grasslands, whilst the Haas model groups these together. Furthermore, WHAM-INFERNO was built using the LUH2 data for anthropogenic land covers (Hurt et al., 2020), whilst the Haas model adopts the ESA CCI remote-sensing product (Li et al., 2018). This led to ontological differences in the treatment of bare soil. Bare soil can have fractional pixel coverage in JULES' vegetation scheme, and is frequently combined with crop PFTs to represent croplands (Burton et al., 2019), whilst in ESA CCI it is a binary class. WHAM! uses the bare soil fraction of a pixel to constrain agent decision making (Perkins et al., 2024a), whilst in the Haas model the cropland land cover class implicitly includes both crops and bare soil present in such land use systems.

Hence, we could not fully reconcile these two approaches. However, it was possible to ensure the scenario anomaly was the same. For anthropogenic land covers, we adopted the LUH2 land cover data across both models. For natural land covers, we used JULES plant functional type (PFT) projections in WHAM-INFERNO and then reconciled JULES PFT projections to the ESA CCI land cover baseline state for the Haas model. As such, we first calculated the natural vegetation coverage for the Haas model as:

$$Natural_{Haas} = Land_{fraction} - Cropland - Urban \quad (3)$$

where $Land_{fraction}$ is the proportion of each pixel covered by land, and $Natural_{Haas}$ is the pixel fraction covered by natural vegetation. As noted above, the Haas model treats pastures as natural grasses and hence they were treated as natural land. We then calculated the fractional composition of natural vegetation in both the ESA CCI data (between forest, shrubs and grasses) and the fractional coverage of the natural JULES PFTs in SSP projections. For the Haas model, the PFTs used were the 9 natural PFTs and 2 pasture PFTs grouped into trees, grasses and shrubs.



Table 2: Model input datasets, source of projections and baseline data for harmonisation. Key: * denotes input data sets used in WHAM! and not in INFERNO; + denotes inputs used by INFERNO but not WHAM! References (where not given): ¹Sellar et al. 2020; ²Lange et al., 2019; ³Mathison et al., 2023; ⁴Hurt et al., 2020; ⁵Hersbach et al., 2020; ⁶Martens et al., 2017; ⁷Wang et al., 2021. ISIMIP3b outputs were those using UK Earth System Model forcings, whilst ISIMIP3a baseline outputs used ERA5 climate inputs.

Variable	WHAM- INFERNO	Haas model	Scenario forcing	Baseline
Air temperature	✓	✓	UKESM ISIMIP3b forcing ^{1,2}	ERA5 ⁵
Precipitation	✓	✓	UKESM ISIMIP3b forcing ^{1,2}	ERA5 ⁵
Atmospheric humidity	✓	✓	UKESM ISIMIP3b forcing ^{1,2}	ERA5 ⁵
Wind speed	✗	✓	UKESM ISIMIP3b forcing ^{1,2}	ERA5 ⁵
Potential evapotranspiration*	✓	✗	JULES ISIMIP3b ³	GLEAM ⁶
Gross primary production	✗	✓	JULES ISIMIP3b ³	MUSES ⁷
Net primary production*	✓	✗	JULES ISIMIP3b ³	MUSES ⁷
Leaf carbon content	✓	✗	JULES ISIMIP3b ³	JULES ISIMIP3a ³
Soil carbon content	✓	✗	JULES ISIMIP3b ³	JULES ISIMIP3a ³
Soil moisture	✓	✗	JULES ISIMIP3b ³	JULES ISIMIP3a ³
Land cover (natural)	✓	✓	JULES ISIMIP3b ³	ESA-CCI ⁸ (Haas) / JULES ISIMIP3a ³ (WHAM-INFERNO)
Land cover (anthropogenic)	✓	✓	LUH2 ⁴	LUH2 ⁴
GDP*	✓	✗	Murakami et al., (2021)	Kummu et al., (2018)
HDI*	✓	✗	Perkins et al., (2024b)	Kummu et al., (2018)
Market access*	✓	✗	Perkins et al., (2024b)	Verburg et al., (2011)
Population density*	✓	✓	Jones and O'Neill, (2016)	CIESIN (2017)
Road density*	✓	✓	Meijer et al., (2018)	Meijer et al., (2018)



We then calculated the annual change in (natural) PFT composition and used this as an anomaly from the ESA CCI baseline state. We multiplied this bias corrected natural land cover composition by the natural fraction derived from LUH2 data (eq 3) to calculate the coverage of natural land cover types. This made the coverage of (natural) PFT i at timestep j :

$$Fraction_{i,j} = \left(\frac{PFT_{i,j}}{\sum PFT_j} - \frac{PFT_{i,1}}{\sum PFT_1} + ESA_frac_i \right) * Natural_{Haas} \quad (4)$$

where $Fraction_{i,j}$ is the coverage of the i th (natural) PFT at timestep j .

2.3 Model experiments & analysis

2.3.1 Model experiments

As well as comparing the respective model outputs for SSP1-2.6 and SSP3-7.0, we explicitly investigate model projections of direct human forcings on burned area. After Burton et al. (2024), we define DHF as the modelled impact of human actions taken at the land surface on burned area. These include land cover change, road building, managed fire use and suppression. DHF is calculated in the models based on the socio-economic scenario forcings in each of the SSPs. Human impacts on climate (and their subsequent impacts on fire), then, are treated separately through the RCPs and associated projections of climate change under differing greenhouse gas concentrations.

Therefore, we ran both models with all scenario forcings variable over time (hereafter “scenario runs”). We then ran a set of experiments with the human forcings held constant at 2020 levels (hereafter “2020 DHF runs”). As the models treat land cover differently, in the 2020 DHF runs, we held cropland constant (as it is treated as an anthropogenic land cover in both models), but allowed other land cover types (grasses, trees, shrubs) to change transiently.

2.3.2 Model output analysis

We used linear correlations to understand the level of agreement between model outputs across the two SSPs, and between baseline runs and 2020 DHF runs. To understand drivers of differences in model projections of DHF we calculated correlations between anthropogenic land cover change (cropland, pasture) and changes in socio-economic forcings (the human development index [HDI], population density) with model projections of DHF.

We then sought to understand whether overall scenario anomalies and anomalies in modelled DHF were predictable based on historical model outputs. Therefore, we calculated model error against GFED5, using outputs for 2011-2014 (the Haas model training period). We calculated model error for each grid cell and calculated mean absolute error by GFED region (Chen et al., 2023). When performing this calculation for GFED regions, we divided errors and future anomaly by the mean GFED5 burned area in each region for the present-day. This accounted for the fact that we would expect model outputs to diverge more in the present in regions with the greatest biophysical capacity to sustain fire.



To assess whether differences in model projections were linked to differences in historical model errors, we calculated linear correlations between absolute differences in model error and absolute differences in future projections. When also sought to identify whether model error against GFED5 followed predictable patterns in line with different levels of human activity. Therefore, we also tested whether differences in absolute model error were linked to differences in socio-economic variables (HDI and population density).

Finally, we calculated the interannual variability (IAV) of model outputs between 2020-2029 and, although a direct evaluation was not possible, we compared this against GFED5 observations between 2011-2020. This was done as models have struggled to reproduce the IAV of historical present-day fire regimes and therefore allows assessment of whether WHAM-INFERNO or the Haas model have improved model capacity to represent this dimension of global fire regimes (Hantson et al., 2020). To account for the human-driven decline in global burned area that is distinct from weather-driven IAV (Andela et al., 2017; Gincheva et al., 2024), we first detrended the GFED5 observations and model outputs using linear models (such that mean BA = 0). We then took the mean of the absolute difference between years as a measure of IAV. Following observational studies (Gincheva et al., 2024; Randerson et al., 2012), we would expect unmanaged wildfires to have a larger interannual variability than managed fires.

3 Results

Future projections from WHAM! have not previously been presented. Therefore, we first present these and their coupling with INFERNO, before comparing outputs with the Haas models. We then focus on understanding the relative impact of DHF across models and scenarios.

3.1 WHAM-INFERNO projections for the Shared Socio-economic Pathways

3.1.1 Managed burned area

WHAM! outputs for managed burned area show sharply differing trends for SSP1-2.6 and SSP3-7.0 (Figure 1). In SSP1-2.6, WHAM! projects that managed burned area will drop to 231 Mha by 2050 and continue to decline to 148 Mha in 2100. By contrast, in SSP3-7.0, global managed fire remains at approximately 2020 levels in 2050 (418 Mha) and declines only to 366 Mha by 2100. In other words, SSP1-2.6 shows an acceleration of observed global declines in managed fire use, whilst SSP3-7.0 sees fire use persist.



The composition and distribution of managed fire also differs between scenarios. WHAM! suggests that pasture management fire (36%) and crop residue burning (CRB; 31%) comprise the largest proportion of human fire use in 2020 (Perkins et al., 2024a). These fire use types decline most strongly in SSP1-2.6, reaching 16% (CRB) and 7% (pasture fire) of managed burned area by 2100 (Figure 2). By contrast, in SSP3-7.0, pasture fire declines modestly as a proportion of managed burned area to 26% in 2100, whilst CRB increases to 37%. For pasture fire, this difference is because of the empirical relationship between economic growth and the replacement of fire-based with machinery-based management in agricultural systems, which is a stronger forcing under SSP1 than SSP3 (Cammelli et al., 2020; Dellink et al., 2017). For crop residue burning, increased yields under intensification empirically produce an initial increase in burning, which then tends to decline under improved environmental and air quality legislation accompanying wider societal development (Millington et al., 2022; Forrest et al., 2024).

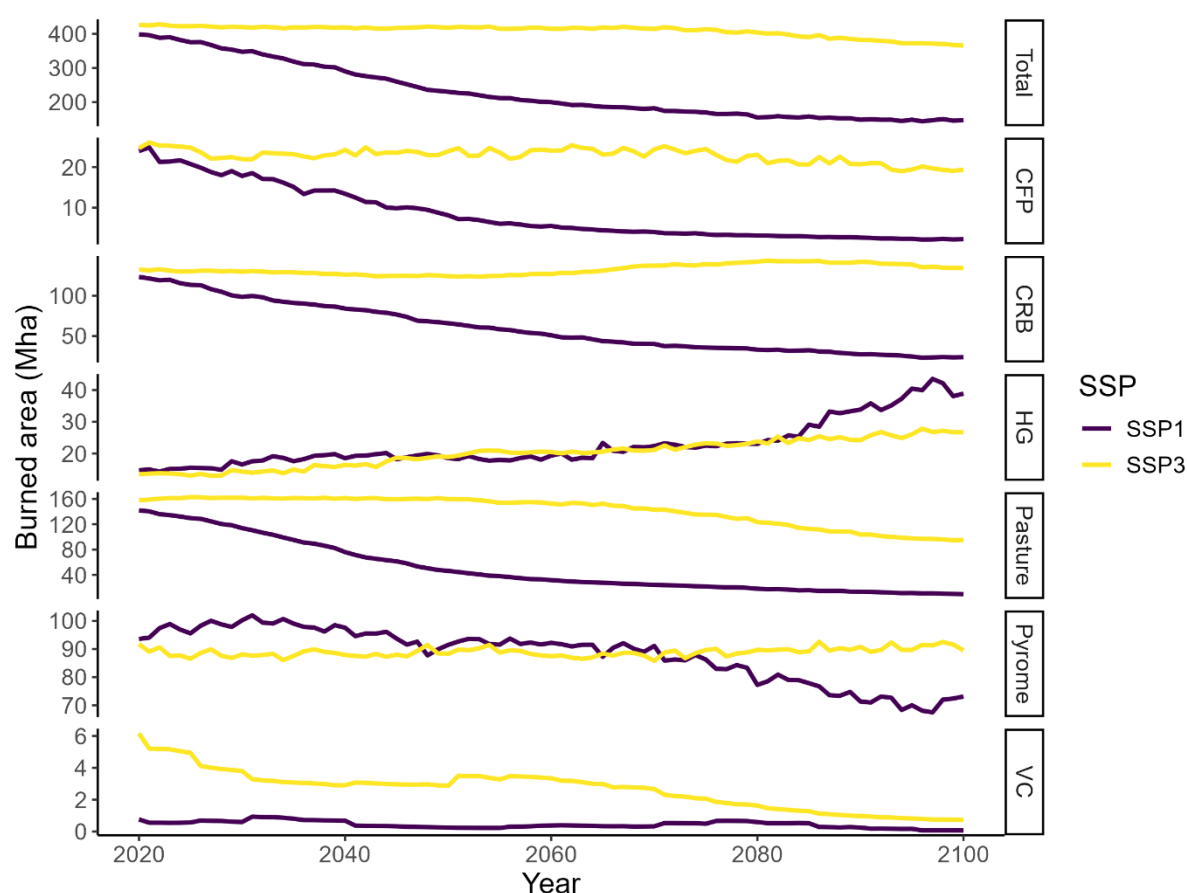
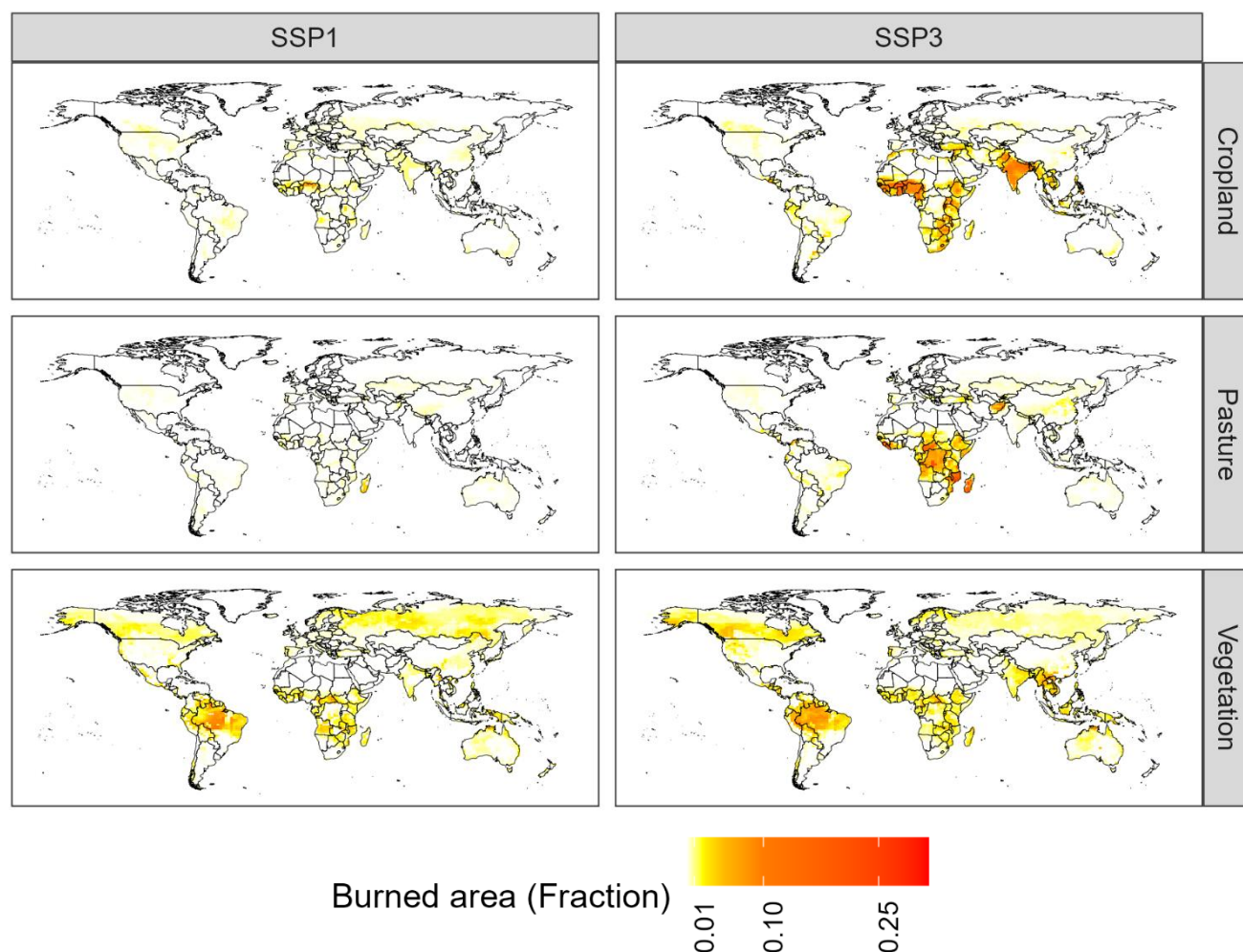


Figure 1: WHAM! projections of managed fire use in the Shared Socio-economic Pathways (SSPs). Agricultural fire uses decline sharply in SSP1 but persist in SSP3. Key: CFP = Crop field preparation; CRB = Crop residue burning; HG = Hunter gatherer; Pyrome = Pyrome management; VC = Vegetation clearance.



270 **Figure 2: WHAM! projections for managed human fire in 2100 under the Shared Socio-economic Pathways (SSPs). Clear**
differences are observed in projected Agriculture and Pasture fires between the SSPs, particularly in Africa and the Indian
subcontinent. Vegetation fire combines crop field preparation, hunter-gatherer fire, pyrome management (fuel load reduction)
and vegetation clearance. A non-linear colour stretch was applied for interpretation.

275



3.1.2 Fire suppression

Fire suppression (active firefighting) increases in both scenarios, reaching a mean value of 0.39 (meaning 39% of unmanaged wildfires are suppressed) in SSP1, and a mean value of 0.29 in SSP3 (Figure 3). Hence, the greater economic development in SSP1 leads WHAM! to project larger increases in suppression, and vice-versa. Beneath this overall pattern, there is some regional heterogeneity. For example, in the eastern USA, suppression intensity is lower in SSP1 than in SSP3 (Figure 4). This occurs as WHAM! projects that such areas begin to adopt a ‘pyro-diverse’ management approach, in which prevention and fuel load reduction through prescribed fire replace intensive firefighting and an overall fire-exclusion strategy (Perkins et al., 2022). The most pronounced differences between SSP1 and SSP3 are in South America, India and eastern China, with the higher socio-economic development in SSP1 leading to higher suppression in each case.

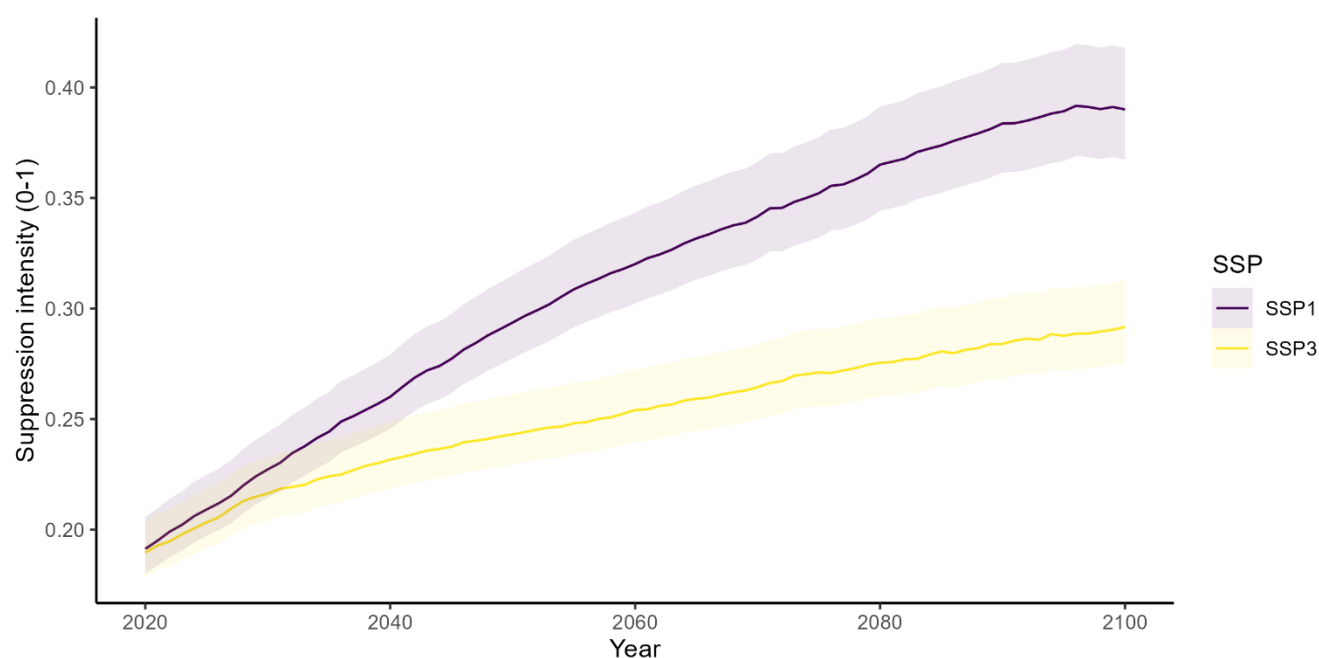


Figure 3: Suppression intensity in WHAM! across Shared Socio-economic Pathways 1 & 3. The shaded area represents the range of outcomes projected by parameter sets identified as pareto optimal during model calibration.

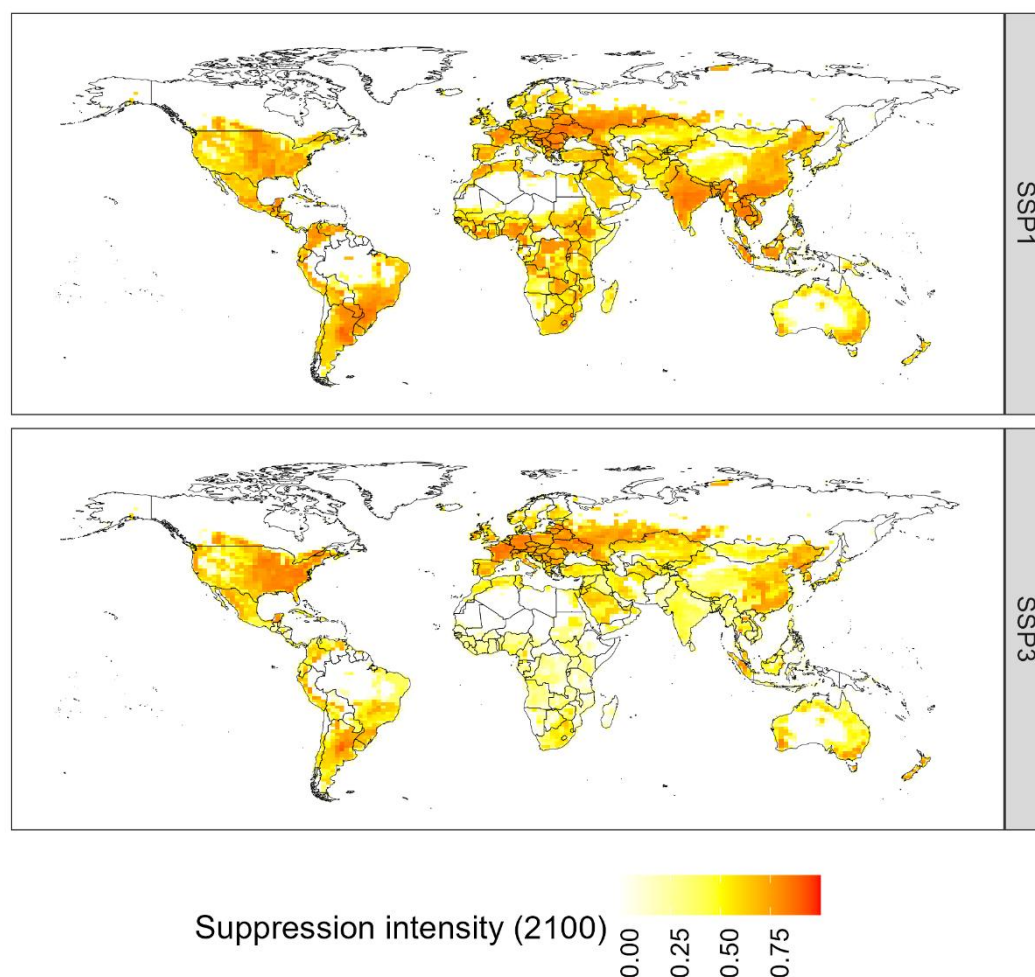


Figure 4: Suppression intensity in WHAM! in 2100 across Shared Socio-economic Pathways 1 & 3. Values shown are the mean of model projections.

295 3.1.3 Coupled WHAM-INFERNO outputs

We briefly describe key trends in coupled WHAM-INFERNO outputs, before presenting more detailed analysis through comparison with outputs from the Haas model in sections 3.2 and 3.3. The WHAM-INFERNO coupled model shows diverging trends in SSPs 1 & 3. In line with declining anthropogenic fire and increased suppression, outputs for SSP1-2.6 suggest a sharp decline in unmanaged fire (Figure 5) reaching a minima of -425 Mha in 2095. By contrast, in line with increased warming, SSP3-7.0 outputs show increased wildfire (120 Mha) leading to an overall increase in burned area of 65 Mha, even as managed fire declines (-55 Mha). As such, in SSP1-2.6, WHAM-INFERNO projects socio-economic change will dominate the effect of climate change, whilst in SSP3-7.0, the effect of climate comes to dominate by 2100.

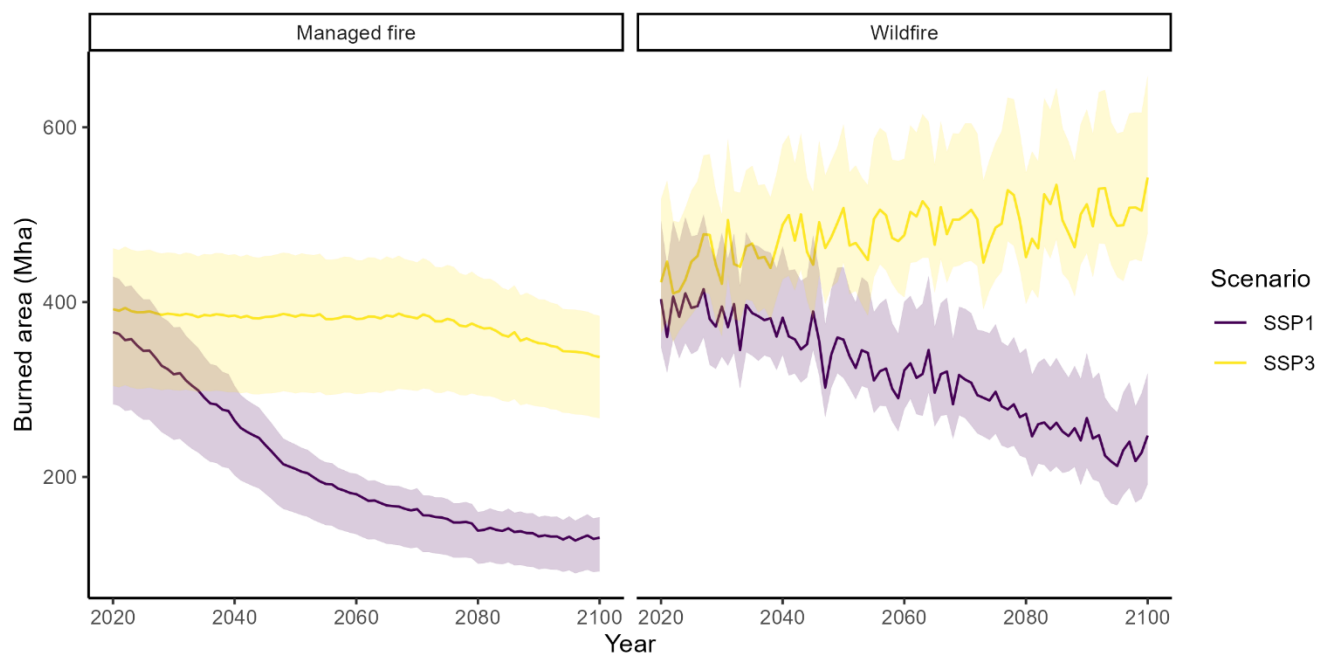


Figure 5: Managed and unmanaged (wildfire) burned area in the Shared Socio-economic Pathways in WHAM-INFERNO. The shaded area represents the range of outcomes projected by parameter sets identified as pareto optimal during model calibration.

3.2 Comparison of WHAM-INFERNO and Haas projections

WHAM-INFERNO and the Haas model provide fundamentally different assessments of the two SSPs (Figure 6). In contrast to WHAM-INFERNO, the Haas model projects little long-term trend in global burned area in SSP1-2.6: the mean burned area from 2020-2030 is 620 Mha compared with 634Mha between 2090-2100. Furthermore, in SSP3-7.0, the Haas model projects a large increase in burned area, peaking at some 1178 Mha in 2098. Overall, therefore, the Haas model projects climate will be the dominant driver of change in global burned area, with its impact dampened by socio-economic forcings in SSP1-2.6. By contrast, WHAM! suggests a dominant role for socio-economic drivers in SSP1-2.6 and a more mixed picture in SSP3-7.0 (Figure 6).

The models have modest agreement about the spatial distribution of change (Figure 7). At the GFED region level, in SSP3-7.0 both models project an increase in burned area in 8 of 15 regions (Figure 8). This includes boreal North America and boreal Asia, where the climate signal is least disrupted by DHF in the present. By contrast, in SSP1 the models disagree on the direction of the trend in 11 of 15 GFED regions. Regions in which models disagree in both scenarios include Central Eastern Asia and Southeast Asia, which currently experience large amounts of agricultural residue burning (Hall et al., 2024; Figure 8). In addition, models disagree in the USA, with WHAM! projecting little change, and the Haas model projecting increases. Notably, dynamic global vegetation models have tended to overestimate burned area in the USA, perhaps due to the omission of the impact of intensive fire suppression policies (Hantson et al., 2020; Kreider et al., 2024; Parks et al., 2025).

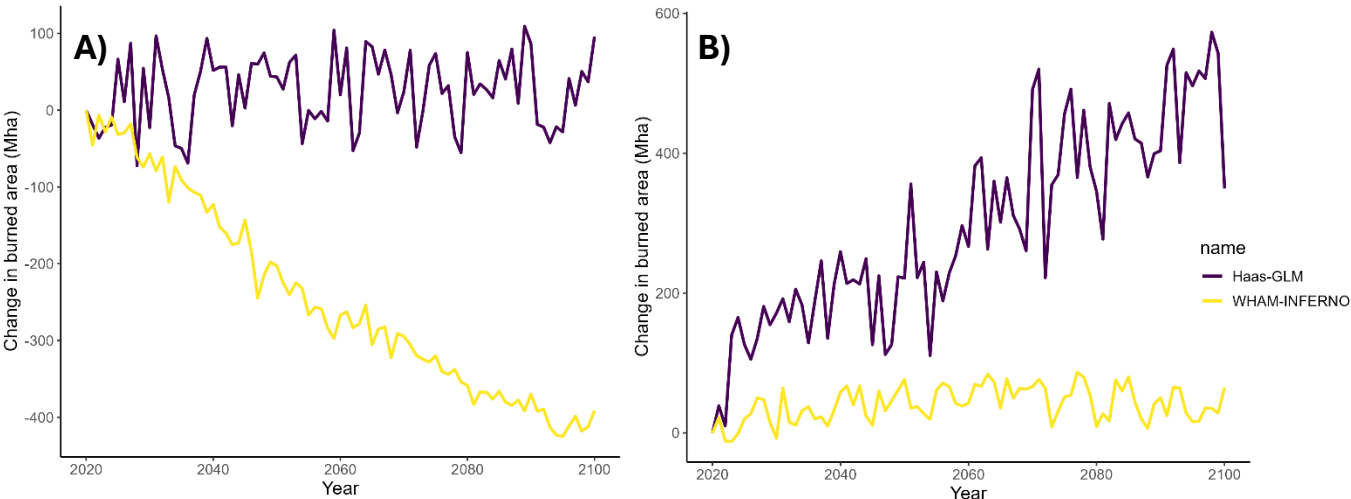
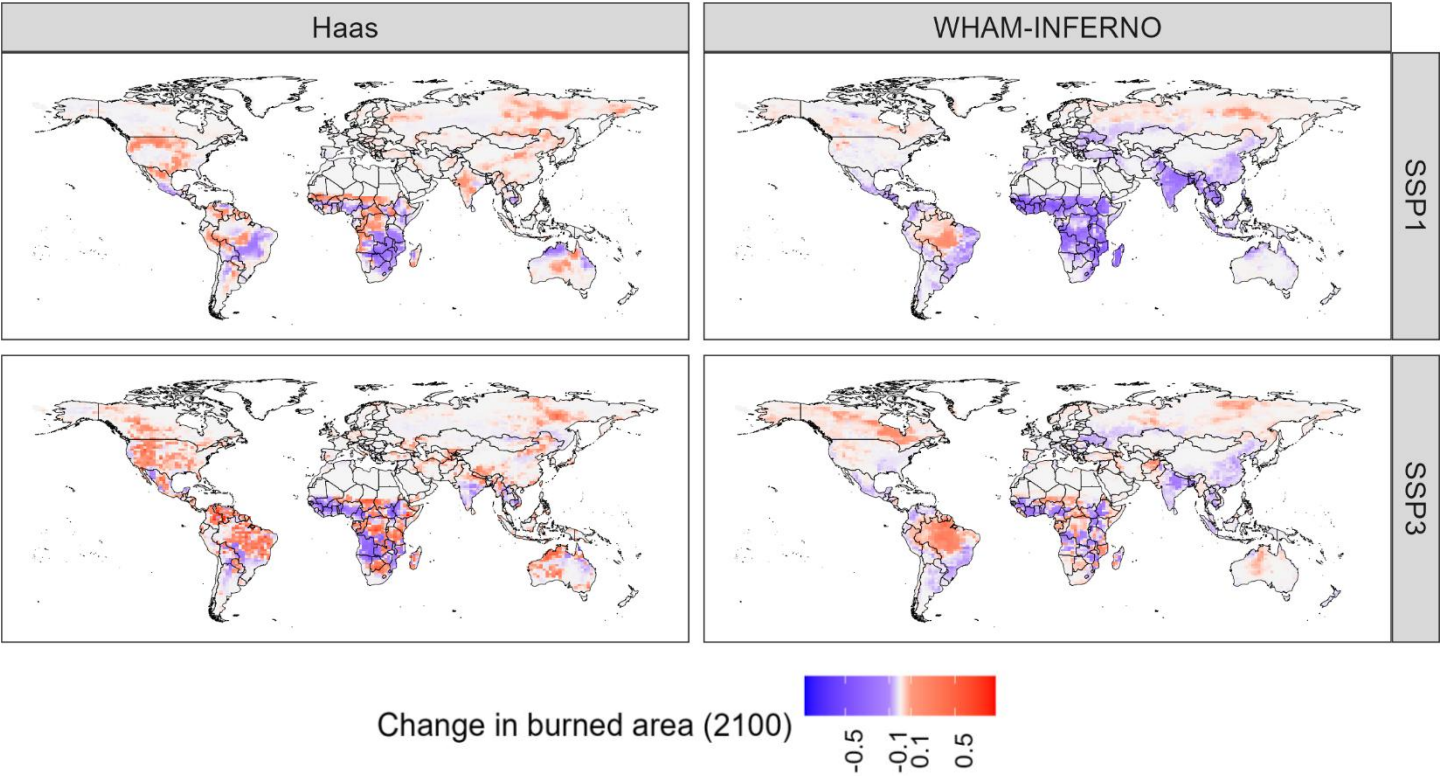


Figure 6: Comparison of burned area anomaly in WHAM-INFERNO and the Haas model for: A) SSP1-2.6; and B) SSP3-7.0.



325 Figure 7: Comparison of burned area anomaly by 2100 between WHAM-INFERNO and the Haas generalised linear model (GLM). WHAM-INFERNO outputs combine managed and unmanaged fire.

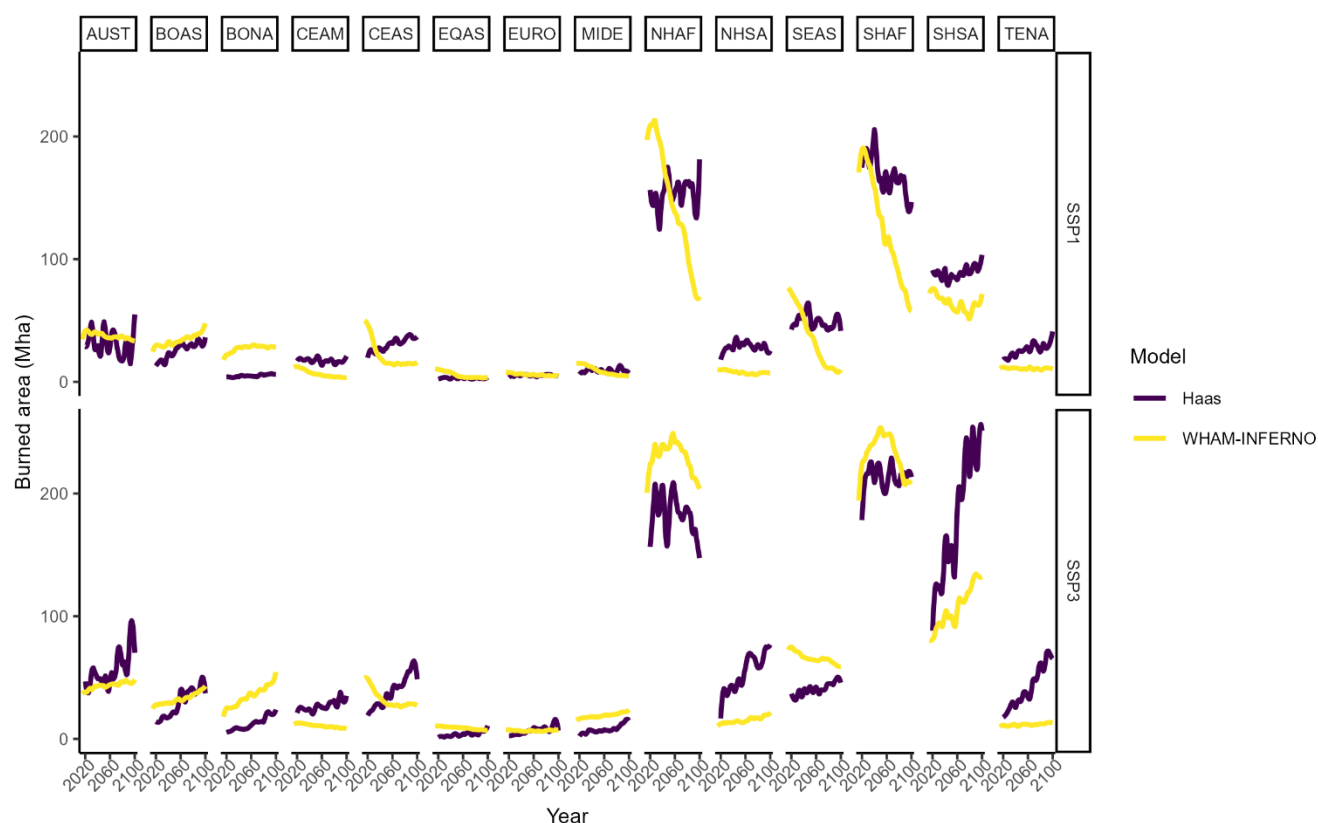


Figure 8: Burned area across the GFED regions. A 1-sigma smoother was applied to Haas model outputs to aid interpretation. **Key:** AUST = Australia, BOAS = Boreal Asia, BONA = Boreal North America, CEAM = Central America & Mexico, CEAS = Central Asia, EQAS = Equatorial Asia, EURO = Europe, MIDE = Middle East & north Africa, NHAF = Northern Hemisphere Africa, NHSA = Northern Hemisphere South America, SEAS = South East Asia, SHAF = Southern Hemisphere Africa, SHSA = Southern Hemisphere South America, TENA = Temperate North America. See Chen et al., (2023) for GFED region boundaries.

There is some evidence that divergence in models' future projections is linked to model error in the present (Figure S1). Perhaps expectedly, model divergence is associated with higher model error in historical runs ($\rho = 0.58$). Similarly, at the GFED region-level, even accounting for the amplitude of present-day burned area, model outputs diverge more where they diverge more in the present ($\rho = 0.67$). Present-day model difference is linked to the human development index (HDI), with WHAM-INFERNO having lower absolute error in GFED regions where HDI is higher, and vice versa ($\rho = 0.45$). However, this pattern is not monotonic, with the Haas model performing better in Australia, a region with high HDI (Figure S2).



Furthermore, the Haas model exhibits higher interannual variability under both scenarios than WHAM-INFERNO. The detrended absolute IAV of the Haas model during 2020-2029 is 61.8 Mha in SSP1 and 40.8 Mha in SSP3-7.0. This compares to 28.5 Mha in GFED5 over 2011-2020. By contrast, WHAM-INFERNO outputs across 2020-2029 have
345 detrended IAV of 23.6 Mha in SSP1-2.6 and 16.6 Mha in SSP3-7.0. As such, although a direct comparison between model outputs and observations was not possible, WHAM-INFERNO seemingly underestimates climate sensitivity, whilst the Haas model may overestimate it. Therefore, for both the spatial distribution and IAV of burned area, the models' future outputs differ in ways that are consistent with their contrasting underlying assumptions. The implications of this are addressed in the discussion.

350 3.3 Impact of direct human forcing

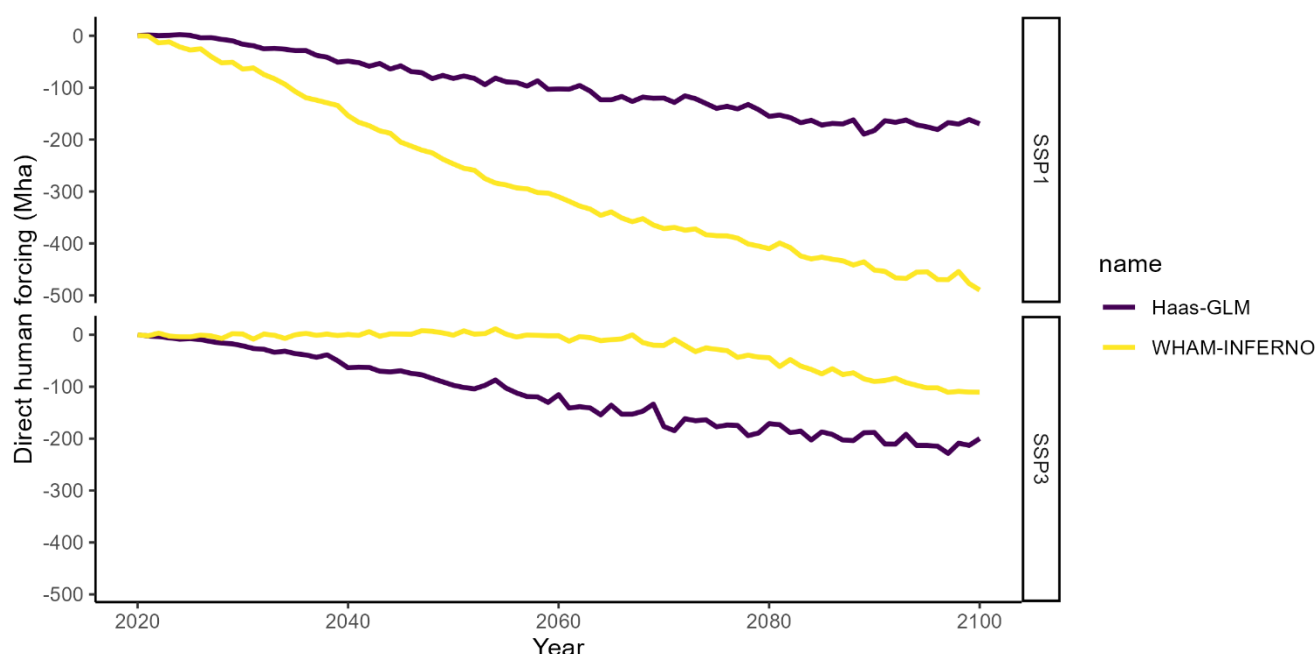
Both models project that the impact of direct human forcing (DHF) on burned area is negative in both SSPs (Figure 9). However, whilst the impact of DHF is approximately equal in SSP1-2.6 and SSP3-7.0 in the Haas model (-170Mha vs -200Mha) there is a sharp divide between SSP1-2.6 and SSP3-7.0 in WHAM-INFERNO (-490Mha vs -111Mha). Indeed, in WHAM-INFERNO in 2050, the modelled impact of DHF in SSP3 is marginally positive (+8Mha) before subsequently
355 becoming negative in 2100. The models' 2100 scenarios are also somewhat more consistent when DHF is held constant ($r = 0.56$), than in baseline model runs with DHF updated dynamically ($r = 0.49$).

The spatial correlation of the two models' projections of DHF is greater between scenarios than between models: Pearson's correlation coefficient between WHAM-INFERNO's projected DHF across SSP1 and SSP3 is 0.52 (Haas SSP1-2.6, SSP3-7.0: $r = 0.39$), compared with a correlation of $r = 0.35$ between WHAM-INFERNO's projected DHF effect and the
360 Haas model's projected DHF (Figure S3). This implies that differences in model structure are at least as important as the scenario forcing in determining future projections of DHF. Notably, the models have much more agreement on the spatial distribution of DHF in SSP1-2.6 ($r = 0.62$) than in SSP3 ($r = 0.15$). This suggests there is greater agreement in determining how DHF will respond to socio-economic development (which dominates SSP1) than to a changing climate (which dominates SSP3). We address the implications of this finding for climate change adaptation in the Discussion.

Underpinning such contrasting projections are different assessments of the processes through which humans directly impact burned area. Notably, the Haas model's projection of DHF is strongly influenced by changes in cropland cover ($r = -0.60$; Figure S4), whilst WHAM-INFERNO has little response ($r = -0.06$). Conversely, WHAM-INFERNO's projected DHF is more sensitive to the Human Development Index ($r = -0.52$) than the Haas model ($r = -0.24$). This is logical, as HDI is an input to WHAM-INFERNO, whilst in the Haas model its impact is only captured implicitly through
370 increased road density. Notably, neither model projects population density as having an overall positive impact on the DHF of burned area (Haas: $r = -0.25$, WHAM-INFERNO: $r = -0.09$).



Finally, whilst the overall impact of DHF in both models is to reduce burned area, both also show areas where DHF increases burned area (Figure 10). WHAM-INFERNO shows a greater extent of increased burned area due to DHF in both
 375 SSP1-2.6 (41 vs 9 Mha) and SSP3-7.0 (111 vs 19 Mha). This occurs primarily because AFTs in WHAM! respond to a warmer climate by increasing pastoral burning (where it remains present) and using fire to manage fuel loads (as represented by pyrome management and hunter-gatherer fire use; Figure 1). This response is widespread in the boreal and Amazon forests, which undergo substantial climate change (Figure 2). Areas of increased burned area due to DHF in WHAM! are most associated with increased pasture ($r = 0.36$) and increased population density ($r = 0.36$). Similarly, increased burned
 380 area due to DHF in the Haas model area is associated with increased pasture ($r = 0.27$; though these are treated as natural grasslands), with a weaker relationship to population density ($r = 0.12$). As WHAM! has explicit representation of crop residue burning, positive DHF of burned area is associated with cropland cover ($r = 0.28$), whilst its impact is always negative in the Haas model ($r = -0.13$).



385 **Figure 9: Impact of direct human forcing (DHF) on burned area anomaly in WHAM-INFERNO and the Haas GLM. DHF represents the difference between model projections with all scenario forcings dynamic, and with DHF held constant at 2020 levels.**

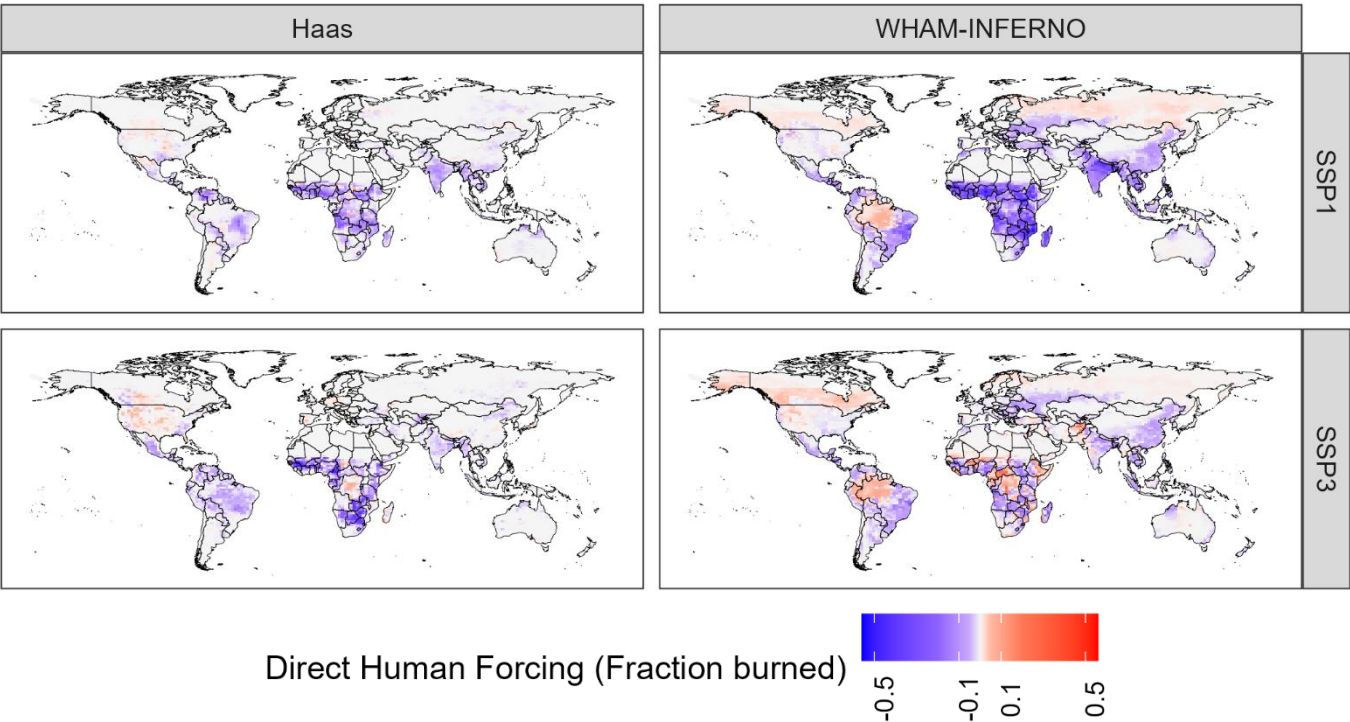


Figure 10: Impact of direct human forcing (DHF) on burned area in 2100. DHF was calculated as the difference between model projections with all scenario forcings dynamic, and with DHF held constant at 2020 levels. A non-linear stretch was applied to the colour-scheme to aid interpretation.

395

4 Discussion

We have presented and compared SSP burned area outputs from WHAM-INFERNO and the Haas GLM. The two models project highly contrasting futures. The Haas model projects higher interannual variability (IAV), increased burned area in SSP3-7.0, and static (though noisy) mean burned area in SSP1-2.6 – indicative of large sensitivity to climate forcings. By contrast, WHAM-INFERNO projects lower IAV, a steep decline in SSP1-2.6, and a modest increase in SSP3-7.0 – indicative of larger sensitivity to socio-economic forcings. Therefore, differences in model output are consistent with the models’ respective underlying assumptions, particularly regarding the direct impacts of humans on burned area. We first discuss the implications of our findings for policy, particularly climate change adaptation, before discussing implications for fire science and modelling.

405



4.1 Implications for policy: adaptation challenges in contrasting futures

Understanding adaptation options in response to a changing climate is a primary challenge for policymakers (Pelling 2011). The presence of a dynamic adaptive response to climate change in WHAM-INFERNO (and its absence in the Haas model), underpins much of the models' differing projections of end-of-century fire regimes. For example, whilst both models suggest
410 that burned area will increase in the boreal forest, in the Haas model this mirrors present-day regimes driven by climate change (Cunningham et al., 2024; Haas et al., 2024). This same warming pattern is represented in WHAM-INFERNO, but occurs alongside a dynamic adaptative response, with increased managed fire used to reduce fuel loads (Figure 7).

Such managed fire use has been widely suggested as a means of adapting to the impacts of climate change (e.g., Oliveras Menor et al., 2025). Consequently, given recent extreme fire years in Canada, support for indigenous-led fire
415 management is gaining pace (Christianson et al., 2022; Hoffman et al., 2022). As noted above, in WHAM-INFERNO, this fire-inclusive ('pyro-diverse') approach to fire management is primarily represented through the 'hunter-gatherer' fire use type, which aims to capture the overall system of indigenous fire management. In highly-developed and fire-prone contexts, this fire inclusive management approach can be supported by state bodies and NGOs (Table S1). This is captured in WHAM! by empirically representing the relationships between the socio-economic and climate conditions that have
420 produced the partnership between state agencies and indigenous groups in the present-day – principally in Northern Australia (Russell-Smith et al., 2015). It is notable, therefore, that hunter-gatherer fire increases more in SSP1-2.6 than SSP3-7.0, even whilst adaptation needs are higher in SSP3-7.0 owing to stronger climate forcing. This trend for stronger adaptive responses under SSP1-2.6 is particularly notable in WHAM! outputs for boreal Russia, an area projected to have substantial increases in burned area under SSP3-7.0 (Figure 2). By contrast, in boreal Canada, the adaptive response is stronger under SSP3-7.0,
425 in line with greater climate forcing. This points to a "soft" limit to adaptation: the modest socio-economic development in SSP3-7.0 entails that WHAM! does not project a return of 'hunter-gatherer' fire in boreal Russia (because lower HDI implies that the conditions needed for successful state partnership with traditional fire users do not occur; Croker et al., 2023). Hence, although SSP1-2.6 has lower climate forcing, WHAM! outputs in this scenario point to a stronger adaptive response.

By contrast, in SSP1, WHAM! points to risks of maladaptation: management decisions that unknowingly
430 exacerbate climate change impacts (Magnan et al., 2016). Perkins et al., (2025a) show that in the present-day, managed human fire use reduces global fire radiative power (FRP) – the amount of energy emitted by a fire and a common proxy variable for fire intensity (Wooster et al., 2005). As such, all else equal, the dramatic reductions in managed human fire use for pasture management and shifting cultivation projected in sub-Saharan Africa, Central and Southern Asia in SSP1, are
435 likely to increase FRP by leaving greater unmanaged fuel loads on the landscape. Given the observed increases in fire intensity with around 1.5°C of warming (Cunningham et al., 2024), the combination of a 2-degree world (implied by RCP 2.6; van Vuuren et al., 2011) and the large reductions in managed fire use projected by WHAM! under SSP1 seems likely to create profound management challenges.



Therefore, an SSP3-7.0 world is likely to create severe adaptation challenges, particularly in regions which
440 experience above average climate warming such as the boreal forest. By contrast, an SSP1-2.6 world will seemingly create
challenges around fire management in the Tropics, particularly how to avoid syndromes of over-suppression, fuel
accumulation and extreme fires currently being experienced in the extra-tropics (Fischer et al., 2016; Hayes, 2021; Moreira
et al., 2020). Both situations could be ameliorated by partnerships between state agencies and indigenous fire users that
enable integrated fire management systems tailored to diverse ecosystems, climates and socio-economic circumstance
445 (Crocker et al., 2023).

4.2 Implications for fire science: understanding fuel load connectivity

Whilst the dynamic human response to climate change may be amongst the most important aspect of our results for policy, it
is also amongst the most uncertain. This uncertainty is rooted in a lack of understanding of the drivers of present-day fire
regimes, and more specifically, in an uncertainty about how impactful managed human fire is on *burned area* (rather than its
450 impact on fire intensity). The Haas model does not include an explicit dynamic human response to climate change and
human impacts on burnt area reflect the indirect effects of changes in cropland, population and road density. There is no
managed fire explicitly represented (Table 1). By contrast, WHAM! represents the hypothesis that human fire use and direct
management are important drivers of global fire regimes (Ford et al., 2021).

Underpinning these different hypotheses is uncertainty about to what extent managed fires fragment fuels, thereby
455 reducing the observed burned area of wildfires. Or posed alternatively, how far removing managed fire would lead to an
increase in burned area from wildfires (Greenwood et al., 2022). Two limitations in WHAM! serve to confound deeper
exploration of this issue. Firstly, different modes of human fire use exhibit different levels of spatial autocorrelation on a
landscape. For example, shifting cultivation and pasture fires may be highly clustered in plots of land close to settlements
and roads (Jakimow et al., 2018; Jakovac et al., 2017). Such fires, if well controlled, may have substantial burned area, but
460 may not reduce or fragment fuel loads outside of a few agricultural areas. By contrast, indigenous fire use in savanna-
grasslands is frequently with the intention of fragmenting fuels across large areas (Bliege Bird et al., 2008). However,
WHAM! does not yet represent the spatial distribution of human fires at any resolution finer than the currently coarse
(~150km²) grid cell size. Secondly, fires used to fragment fuels (pyrome management in Figure 1) are often set early in the
dry season to prevent very large and intense late dry season fires (Laris, 2002). However, WHAM! does not yet represent
465 fire use seasonality and so cannot capture this difference.

To some extent, such complications may be addressed by an online coupling of WHAM! with JULES-INFERNO,
which would enable dynamic feedback between human fire use and vegetation (this coupling work is in progress; Perkins et
al., 2025c). However, in practice, this is unlikely to fully capture the sub-pixel distribution of different forms of fire and their
respective impact on vegetation connectivity. Rather, uncertainties around the spatiotemporal distribution of managed fire at
470 sub-pixel scale (i.e., here < c.150km²) combine with uncertainties around other anthropogenic and natural drivers of fuel
fragmentation. For example, managed human fires are generally cooler and less intense than unmanaged wildfires, which



will impact rates of post-fire regrowth, and hence the ability of an ecosystem to sustain subsequent fires (Coppoletta et al., 2016; Maia et al., 2012). Over prolonged periods, application of managed fire will likely lead to profound changes in ecosystems that evolved under a fire regime governed by rare, intense, and lightning-ignited fires (Keeley and Pausas, 2022).

475 Furthermore, human fire use interacts not only with ecological heterogeneity, but also heterogeneity in other anthropogenic fragmentation processes. For example, WHAM! adopts the Haas hypothesis that road density is an important constraint on fire size, and models fire size as exponentially decaying with increased road density (Perkins et al., 2025a). However, this is a somewhat limited, top-down view of fragmentation that assumes road density has a universal suppressive effect, and should be improved through consideration of interactions between differing fragmentation drivers (Bowring et al.,
480 2024; Chas-Amil et al., 2013; Driscoll et al., 2021). Even at a simple level, it does not account for varying road types: multi-lane motorways and dirt tracks are treated as equivalent. Future research could therefore seek to incorporate explicit parameterisation of road type into fire models (data which are captured by Meijer et al., 2018).

Fire-vegetation feedbacks are also a limitation of the Haas model, which does not account for the influence of previous burning on current vegetation. Including such feedbacks could have a significant effect on model projections,
485 including by dampening interannual variability, whilst maintaining the current model assumptions about DHF. In addition, when run under dramatically different forcings (of similar magnitude of change to SSP3-7.0) at the Last Glacial Maximum, the model was able to capture the overall sign of change in burnt area compared to the charcoal record (Haas et al., 2023). This out-of-sample experiment provides some reassurance as to the ability of the model to capture the response of burnt area to the climate signal. Nevertheless, the ability of the model to capture DHF has not been evaluated and could dramatically
490 influence future projections.

Overall, understanding how human fire use interacts with wider anthropogenic fragmentation across different ecosystems represents a major challenge in fire science. Promising ways forward include observational studies of factors that constrain fire spread, such as that of Janssen and Veraverbeke (2025) in the boreal forest. This approach could be replicated in tropical savanna landscapes and others with higher levels of human perturbation, and could perhaps be complemented
495 with reduced complexity modelling to develop and test hypotheses of constraints on fire spread across different ecosystems and socio-economic contexts (Archibald et al., 2012; Malamud et al., 1998).

4.3 Implications for modelling: navigating structural uncertainty

Comparison of modelled DHF between the Haas model and WHAM-INFERNO revealed that differences between models were greater than those between scenarios. This finding is similar to that of Alexander et al., (2017), who found that different
500 approaches to representing human decision-making in models of land use change (e.g., agent-based, least-cost optimisation) had a greater impact than scenario forcing on model outputs. A similar finding was also produced by Brown et al., (2021) in the context of land use change in Europe. This is not to say that uncertainties in scenario forcings do not shape model outputs: for example, projections here for the Haas model and those presented in Haas et al., (2024) are notably different across the Amazon, where the UKESM projects earlier and more rapid change than other Earth system models (Drijfhout et



505 al., 2015). Nevertheless, it is seemingly a property of spatial modelling of socio-ecological systems that models are extremely sensitive to the way in which human decision making is represented.

In the case of land use change modelling, such differences reflect differing model purposes and perhaps irreconcilable theories of economic behaviour (e.g., utility maximisation versus satisficing; Groeneveld et al., 2017). However, the two models presented here do not appear irreconcilable. For example, in common with many process-based
510 fire models, WHAM-INFERNO's modest increase in burned area in SSP3 and low IAV suggests it is likely under-sensitive to climate forcings (Hantson et al., 2020). Indeed during calibration, it was found to have this limitation (Perkins et al., 2025a). By contrast, the Haas model's seeming overestimation of IAV may mean it underestimates the effect of DHF.

As such, our assessment is that each model has advanced on previous understanding of the processes driving global burned area within its domain, but both also remain incomplete. Therefore, the insights from the two models could be
515 combined towards a new generation of coupled socio-ecological fire models. For example, such models could draw on insights from the Haas models including the central role of GPP in fire regimes, and how the biophysical-drivers of burned area differ from fire intensity (Haas et al., 2022). This could be combined with WHAM-INFERNO's representation of DHF and dynamic human adaptation. Critical to the success of such models would be tackling issues of fuel-load connectivity, as discussed above.

520 At the same time, the modest performance of process-based fire models in reproducing observations has given rise to deep-learning-based fire models as an alternative approach (Guo et al., 2025; Son et al., 2024). This is a broadly welcome step, particularly for fire risk forecasting and management (Cheng et al., 2022; Son et al., 2022), but results here should also give pause for thought for projections over longer timescales. The Haas model and WHAM-INFERNO can both approximately equally reproduce historical observations (Figure S1 & S2), yet do so with fundamentally different
525 conceptualisation and representation of core processes. Consequently, projections from modelling methods that can have challenges with overfitting to noise, need to be treated with caution (Reichstein et al., 2019; Rocks and Mehta, 2022). In common with many environmental processes, there is still a comparatively short observational record of burned area (especially at fine spatial scales commensurate with much human fire use), and the socio-ecological conditions under which we wish to understand possible fire regimes differ greatly from the present-day (Haas et al., 2023; Schneider et al., 2024).
530 Close collaboration between process-based and machine-learning modellers is likely to lead to optimal outcomes for both understanding and prediction of future fire regimes (Huang et al., 2024; Lampe et al., 2025).



5 Conclusion

We have presented future projections of the WHAM! agent-based model coupled to the INFERNO biophysical fire model and compared these with the Haas generalised linear model of burned area. The models represent contrasting hypotheses about the drivers of global fire regimes. Consequently, they produce extremely different futures for the same scenarios yet do so in ways that are consistent with their underlying assumptions. We conclude that combining insights from both models is likely to prove a fruitful avenue for advancing global fire science. A critical disagreement between the models concerns how humans will respond and adapt to climate change. The WHAM-INFERNO ensemble demonstrates the potential for coupled human-Earth system models to explore both limits to adaptation and possible maladaptation under diverse futures. However, the differences in model representation of such processes also highlights large structural uncertainties. Future model development will need to grapple with these questions as adaptation becomes an ever-increasing policy challenge.

Author contribution

All authors contributed to study conceptualisation and methodology. OP & OH conducted data curation; OP conducted formal analysis. JDAM provided project supervision. AV acquired funding. OP & JDAM wrote the original draft. All authors reviewed and revised the draft.

Code and data availability

Data and code to reproduce the results presented here are made available as Perkins et al., (2025b), <https://zenodo.org/records/16635274>.

550 Competing interests

The authors declare they have no conflict of interests.

Funding

This work was funded by the Leverhulme Centre for Wildfires, Environment and Society through the Leverhulme Trust, Grant RC-2018-023. AV has also been supported by the AXA Research Fund (project “AXA Chair in Wildfires and Climate”) and
555 by the Hellenic Foundation for Research and Innovation (Grant 3453).



References

- Alexander, P., Prestele, R., Verburg, P.H., Arneth, A., Baranzelli, C., Batista e Silva, F., Brown, C., Butler, A., Calvin, K., Dendoncker, N., Doelman, J.C., Dunford, R., Engström, K., Eitelberg, D., Fujimori, S., Harrison, P.A., Hasegawa, T., Havlik, P., Holzhauser, S., Humpenöder, F., Jacobs-Crisioni, C., Jain, A.K., Krisztin, T., Kyle, P., Laval, C., Lenton, T., Liu, J., Meiyappan, P., Popp, A., Powell, T., Sands, R.D., Schaldach, R., Stehfest, E., Steinbuks, J., Tabeau, A., van Meijl, H., Wise, M.A., Rounsevell, M.D.A., 2017. Assessing uncertainties in land cover projections. *Global Change Biology* 23, 767–781. <https://doi.org/10.1111/gcb.13447>.
- Andela, N., Morton, D.C., Giglio, L., Chen, Y., van der Werf, G.R., Kasibhatla, P.S., DeFries, R.S., Collatz, G.J., Hantson, S., Kloster, S., Bachelet, D., Forrest, M., Lasslop, G., Li, F., Mangeon, S., Melton, J.R., Yue, C., Randerson, J.T., 2017. A human-driven decline in global burned area. *Science* 356, 1356–1362. <https://doi.org/10.1126/science.aal4108>.
- Archibald, S., Lehmann, C.E.R., Gómez-Dans, J.L., Bradstock, R.A., 2013. Defining pyromes and global syndromes of fire regimes. *Proceedings of the National Academy of Sciences* 110, 6442–6447. <https://doi.org/10.1073/pnas.1211466110>.
- Archibald, S., Staver, A.C., Levin, S.A., 2012. Evolution of human-driven fire regimes in Africa. *Proceedings of the National Academy of Sciences* 109, 847–852. <https://doi.org/10.1073/pnas.1118648109>.
- Armstrong McKay, D.I., Staal, A., Abrams, J.F., Winkelmann, R., Sakschewski, B., Loriani, S., Fetzer, I., Cornell, S.E., Rockström, J., Lenton, T.M., 2022. Exceeding 1.5°C global warming could trigger multiple climate tipping points. *Science* 377, eabn7950. <https://doi.org/10.1126/science.abn7950>.
- Arneth, A., Brown, C., Rounsevell, M.D.A., 2014. Global models of human decision-making for land-based mitigation and adaptation assessment. *Nature Clim Change* 4, 550–557. <https://doi.org/10.1038/nclimate2250>.
- Bliege Bird, R., Bird, D.W., Coddig, B.F., Parker, C.H., Jones, J.H., 2008. The “fire stick farming” hypothesis: Australian Aboriginal foraging strategies, biodiversity, and anthropogenic fire mosaics. *Proceedings of the National Academy of Sciences* 105, 14796–14801. <https://doi.org/10.1073/pnas.0804757105>.
- Bowring, S.P.K., Li, W., Mouillot, F., Rosan, T.M., Ciais, P., 2024. Road fragment edges enhance wildfire incidence and intensity, while suppressing global burned area. *Nat Commun* 15, 9176. <https://doi.org/10.1038/s41467-024-53460-6>.
- Brown, C., Holman, I., Rounsevell, M., 2021. How modelling paradigms affect simulated future land use change. *Earth System Dynamics* 12, 211–231. <https://doi.org/10.5194/esd-12-211-2021>.
- Burton, C., Betts, R., Cardoso, M., Feldpausch, T.R., Harper, A., Jones, C.D., Kelley, D.I., Robertson, E., Wiltshire, A., 2019. Representation of fire, land-use change and vegetation dynamics in the Joint UK Land Environment Simulator vn4.9 (JULES). *Geoscientific Model Development* 12, 179–193. <https://doi.org/10.5194/gmd-12-179-2019>.
- Burton, C., Lampe, S., Kelley, D.I., Thiery, W., Hantson, S., Christidis, N., Gudmundsson, L., Forrest, M., Burke, E., Chang, J., Huang, H., Ito, A., Kou-Giesbrecht, S., Lasslop, G., Li, W., Nieradzik, L., Li, F., Chen, Y., Randerson, J., Reyer, C.P.O., Mengel, M., 2024. Global burned area increasingly explained by climate change. *Nat. Clim. Chang.* 14, 1186–1192. <https://doi.org/10.1038/s41558-024-02140-w>.



- 590 Cammelli, F., Garrett, R.D., Barlow, J., Parry, L., 2020. Fire risk perpetuates poverty and fire use among Amazonian smallholders. *Global Environmental Change* 63, 102096. <https://doi.org/10.1016/j.gloenvcha.2020.102096>.
- Cano-Crespo, A., Oliveira, P.J.C., Boit, A., Cardoso, M., Thonicke, K., 2015. Forest edge burning in the Brazilian Amazon promoted by escaping fires from managed pastures. *Journal of Geophysical Research: Biogeosciences* 120, 2095–2107. <https://doi.org/10.1002/2015JG002914>.
- 595 Chas-Amil, M.L., Touza, J., García-Martínez, E., 2013. Forest fires in the wildland–urban interface: A spatial analysis of forest fragmentation and human impacts. *Applied Geography* 43, 127–137. <https://doi.org/10.1016/j.apgeog.2013.06.010>.
- Chen, Y., Hall, J., van Wees, D., Andela, N., Hantson, S., Giglio, L., van der Werf, G.R., Morton, D.C., Randerson, J.T., 2023. Multi-decadal trends and variability in burned area from the fifth version of the Global Fire Emissions Database (GFED5). *Earth System Science Data* 15, 5227–5259. <https://doi.org/10.5194/essd-15-5227-2023>.
- 600 Cheng, S., Jin, Y., Harrison, S.P., Quilodrán-Casas, C., Prentice, I.C., Guo, Y.-K., Arcucci, R., 2022. Parameter Flexible Wildfire Prediction Using Machine Learning Techniques: Forward and Inverse Modelling. *Remote Sensing* 14, 3228. <https://doi.org/10.3390/rs14133228>.
- Christianson, A.C., Sutherland, C.R., Moola, F., Gonzalez Bautista, N., Young, D., MacDonald, H., 2022. Centering Indigenous Voices: The Role of Fire in the Boreal Forest of North America. *Curr Forestry Rep* 8, 257–276. <https://doi.org/10.1007/s40725-022-00168-9>.
- 605 Center for International Earth Science Information Network (CIESIN), 2017. Gridded Population of the World, Version 4 (GPWv4): Population Density. <https://doi.org/10.7927/H49C6VHW>.
- Coppoletta, M., Merriam, K.E., Collins, B.M., 2016. Post-fire vegetation and fuel development influences fire severity patterns in reburns. *Ecological Applications* 26, 686–699. <https://doi.org/10.1890/15-0225>.
- 610 Croker, A.R., Woods, J., Kountouris, Y., 2023. Community-Based Fire Management in East and Southern African Savanna-Protected Areas: A Review of the Published Evidence. *Earth's Future* 11, e2023EF003552. <https://doi.org/10.1029/2023EF003552>.
- Cunningham, C.X., Williamson, G.J., Bowman, D.M.J.S., 2024. Increasing frequency and intensity of the most extreme wildfires on Earth. *Nat Ecol Evol* 8, 1420–1425. <https://doi.org/10.1038/s41559-024-02452-2>.
- 615 Dellink, R., Chateau, J., Lanzi, E., Magné, B., 2017. Long-term economic growth projections in the Shared Socio-economic Pathways. *Global Environmental Change* 42, 200–214. <https://doi.org/10.1016/j.gloenvcha.2015.06.004>.
- Drijfhout, S., Bathiany, S., Beaulieu, C., Brovkin, V., Claussen, M., Huntingford, C., Scheffer, M., Sgubin, G., Swingedouw, D., 2015. Catalogue of abrupt shifts in Intergovernmental Panel on Climate Change climate models. *Proceedings of the National Academy of Sciences* 112, E5777–E5786. <https://doi.org/10.1073/pnas.1511451112>.
- 620 Driscoll, D.A., Armenteras, D., Bennett, A.F., Brotons, L., Clarke, M.F., Doherty, T.S., Haslem, A., Kelly, L.T., Sato, C.F., Sitters, H., Aquilué, N., Bell, K., Chadid, M., Duane, A., Meza-Elizalde, M.C., Giljohann, K.M., González, T.M., Jambhekar, R., Lazzari, J., Morán-Ordóñez, A., Wevill, T., 2021. How fire interacts with habitat loss and fragmentation. *Biological Reviews* 96, 976–998. <https://doi.org/10.1111/brv.12687>.



- Fischer, A.P., Spies, T.A., Steelman, T.A., Moseley, C., Johnson, B.R., Bailey, J.D., Ager, A.A., Bourgeron, P., Charnley, S., Collins, B.M., Kline, J.D., Leahy, J.E., Littell, J.S., Millington, J.D., Nielsen-Pincus, M., Olsen, C.S., Paveglio, T.B., Roos, C.I., Steen-Adams, M.M., Stevens, F.R., Vukomanovic, J., White, E.M., Bowman, D.M., 2016. Wildfire risk as a socioecological pathology. *Frontiers in Ecology and the Environment* 14, 276–284. <https://doi.org/10.1002/fee.1283>.
- Ford, A.E.S., Harrison, S.P., Kountouris, Y., Millington, J.D.A., Mistry, J., Perkins, O., Rabin, S.S., Rein, G., Schreckenberger, K., Smith, C., Smith, T.E.L., Yadav, K., 2021. Modelling Human-Fire Interactions: Combining Alternative Perspectives and Approaches. *Front. Environ. Sci.* 9. <https://doi.org/10.3389/fenvs.2021.649835>.
- Forrest, M., Hetzer, J., Billing, M., Bowring, S.P.K., Kosczor, E., Oberhagemann, L., Perkins, O., Warren, D., Arrogante-Funes, F., Thonicke, K., Hickler, T., 2024. Understanding and simulating cropland and non-cropland burning in Europe using the BASE (Burnt Area Simulator for Europe) model. *Biogeosciences* 21, 5539–5560. <https://doi.org/10.5194/bg-21-5539-2024>.
- Frieler, K., Lange, S., Piontek, F., Reyer, C.P.O., Schewe, J., Warszawski, L., Zhao, F., Chini, L., Denvil, S., Emanuel, K., Geiger, T., Halladay, K., Hurtt, G., Mengel, M., Murakami, D., Ostberg, S., Popp, A., Riva, R., Stevanovic, M., Suzuki, T., Volkholz, J., Burke, E., Ciais, P., Ebi, K., Eddy, T.D., Elliott, J., Galbraith, E., Gosling, S.N., Hattermann, F., Hickler, T., Hinkel, J., Hof, C., Huber, V., Jägermeyr, J., Krysanova, V., Marcé, R., Müller Schmied, H., Mouratiadou, I., Pierson, D., Tittensor, D.P., Vautard, R., van Vliet, M., Biber, M.F., Betts, R.A., Bodirsky, B.L., Deryng, D., Froliking, S., Jones, C.D., Lotze, H.K., Lotze-Campen, H., Sahajpal, R., Thonicke, K., Tian, H., Yamagata, Y., 2017. Assessing the impacts of 1.5 °C global warming – simulation protocol of the Inter-Sectoral Impact Model Intercomparison Project (ISIMIP2b). *Geoscientific Model Development* 10, 4321–4345. <https://doi.org/10.5194/gmd-10-4321-2017>.
- Frieler, K., Volkholz, J., Lange, S., Schewe, J., Mengel, M., del Rocío Rivas López, M., Otto, C., Reyer, C.P.O., Karger, D.N., Malle, J.T., Treu, S., Menz, C., Blanchard, J.L., Harrison, C.S., Petrik, C.M., Eddy, T.D., Ortega-Cisneros, K., Novaglio, C., Rousseau, Y., Watson, R.A., Stock, C., Liu, X., Heneghan, R., Tittensor, D., Maury, O., Büchner, M., Vogt, T., Wang, T., Sun, F., Sauer, I.J., Koch, J., Vanderkelen, I., Jägermeyr, J., Müller, C., Rabin, S., Klar, J., Vega del Valle, I.D., Lasslop, G., Chadburn, S., Burke, E., Gallego-Sala, A., Smith, N., Chang, J., Hantson, S., Burton, C., Gädeke, A., Li, F., Gosling, S.N., Müller Schmied, H., Hattermann, F., Wang, J., Yao, F., Hickler, T., Marcé, R., Pierson, D., Thiery, W., Mercado-Bettín, D., Ladwig, R., Ayala-Zamora, A.I., Forrest, M., Bechtold, M., 2024. Scenario setup and forcing data for impact model evaluation and impact attribution within the third round of the Inter-Sectoral Impact Model Intercomparison Project (ISIMIP3a). *Geoscientific Model Development* 17, 1–51. <https://doi.org/10.5194/gmd-17-1-2024>.
- Giglio, L., Randerson, J.T., van der Werf, G.R., 2013. Analysis of daily, monthly, and annual burned area using the fourth-generation global fire emissions database (GFED4). *Journal of Geophysical Research: Biogeosciences* 118, 317–328. <https://doi.org/10.1002/jgrg.20042>.
- Gincheva, A., Pausas, J.G., Torres-Vázquez, M.Á., Bedia, J., Vicente-Serrano, S.M., Abatzoglou, J.T., Sánchez-Espigares, J.A., Chuvieco, E., Jerez, S., Provenzale, A., Trigo, R.M., Turco, M., 2024. The Interannual Variability of Global Burned Area Is Mostly Explained by Climatic Drivers. *Earth's Future* 12, e2023EF004334. <https://doi.org/10.1029/2023EF004334>.



- Greenwood, L., Bliege Bird, R., Nimmo, D., 2022. Indigenous burning shapes the structure of visible and invisible fire mosaics. *Landsc Ecol* 37, 811–827. <https://doi.org/10.1007/s10980-021-01373-w>.
- 660 Groeneveld, J., Müller, B., Buchmann, C.M., Dressler, G., Guo, C., Hase, N., Hoffmann, F., John, F., Klassert, C., Lauf, T., Liebelt, V., Nolzen, H., Pannicke, N., Schulze, J., Weise, H., Schwarz, N., 2017. Theoretical foundations of human decision-making in agent-based land use models – A review. *Environmental Modelling & Software* 87, 39–48. <https://doi.org/10.1016/j.envsoft.2016.10.008>.
- Guo, Z., Li, W., Ciais, P., Sitch, S., van der Werf, G.R., Bowring, S.P.K., Bastos, A., Mouillot, F., He, J., Sun, M., Zhu, L.,
- 665 Du, X., Wang, N., Huang, X., 2025. Reconstructed global monthly burned area maps from 1901 to 2020. *Earth System Science Data Discussions* 1–28. <https://doi.org/10.5194/essd-2024-556>.
- Haas, O., Prentice, I., Harrison, S., 2024. Global wildfires on a changing planet. <https://doi.org/10.21203/rs.3.rs-4359943/v1>
- Haas, O., Prentice, I.C., Harrison, S.P., 2023. The response of wildfire regimes to Last Glacial Maximum carbon dioxide and climate. *Biogeosciences* 20, 3981–3995. <https://doi.org/10.5194/bg-20-3981-2023>.
- 670 Haas, O., Prentice, I.C., Harrison, S.P., 2022. Global environmental controls on wildfire burnt area, size, and intensity. *Environ. Res. Lett.* 17, 065004. <https://doi.org/10.1088/1748-9326/ac6a69>.
- Hall, J.V., Argueta, F., Zubkova, M., Chen, Y., Randerson, J.T., Giglio, L., 2024. GloCAB: global cropland burned area from mid-2002 to 2020. *Earth System Science Data* 16, 867–885. <https://doi.org/10.5194/essd-16-867-2024>.
- Hantson, S., Kelley, D.I., Arneth, A., Harrison, S.P., Archibald, S., Bachelet, D., Forrest, M., Hickler, T., Lasslop, G., Li, F.,
- 675 Mangeon, S., Melton, J.R., Nieradzick, L., Rabin, S.S., Prentice, I.C., Sheehan, T., Sitch, S., Teckentrup, L., Voulgarakis, A., Yue, C., 2020. Quantitative assessment of fire and vegetation properties in simulations with fire-enabled vegetation models from the Fire Model Intercomparison Project. *Geoscientific Model Development* 13, 3299–3318. <https://doi.org/10.5194/gmd-13-3299-2020>.
- Harrison, S.P., Prentice, I.C., Bloomfield, K.J., Dong, N., Forkel, M., Forrest, M., Ningthoujam, R.K., Pellegrini, A., Shen,
- 680 Y., Baudena, M., Cardoso, A.W., Huss, J.C., Joshi, J., Oliveras, I., Pausas, J.G., Simpson, K.J., 2021. Understanding and modelling wildfire regimes: an ecological perspective. *Environ. Res. Lett.* 16, 125008. <https://doi.org/10.1088/1748-9326/ac39be>.
- Hayes, J.P., 2021. Fire Suppression and the Wildfire Paradox in Contemporary China: Policies, Resilience, and Effects in Chinese Fire Regimes. *Hum Ecol* 49, 19–32. <https://doi.org/10.1007/s10745-020-00183-z>.
- 685 Hersbach, H., Bell, B., Berrisford, P., Hirahara, S., Horányi, A., Muñoz-Sabater, J., Nicolas, J., Peubey, C., Radu, R., Schepers, D., Simmons, A., Soci, C., Abdalla, S., Abellan, X., Balsamo, G., Bechtold, P., Biavati, G., Bidlot, J., Bonavita, M., De Chiara, G., Dahlgren, P., Dee, D., Diamantakis, M., Dragani, R., Flemming, J., Forbes, R., Fuentes, M., Geer, A., Haimberger, L., Healy, S., Hogan, R.J., Hólm, E., Janisková, M., Keeley, S., Laloyaux, P., Lopez, P., Lupu, C., Radnoti, G., de Rosnay, P., Rozum, I., Vamborg, F., Villaume, S., Thépaut, J.-N., 2020. The ERA5 global reanalysis. *Quarterly Journal*
- 690 *of the Royal Meteorological Society* 146, 1999–2049. <https://doi.org/10.1002/qj.3803>.



- Hoffman, K.M., Christianson, A.C., Dickson-Hoyle, S., Copes-Gerbitz, K., Nikolakis, W., Diabo, D.A., McLeod, R., Michell, H.J., Mamun, A.A., Zahara, A., Mauro, N., Gilchrist, J., Ross, R.M., Daniels, L.D., 2022. The right to burn: barriers and opportunities for Indigenous-led fire stewardship in Canada. *FACETS* 7, 464–481. <https://doi.org/10.1139/facets-2021-0062>.
- 695 Huang, G., Wang, Y., Ham, Y.-G., Mu, B., Tao, W., Xie, C., 2024. Toward a Learnable Climate Model in the Artificial Intelligence Era. *Adv. Atmos. Sci.* 41, 1281–1288. <https://doi.org/10.1007/s00376-024-3305-9>.
- Hurt, G.C., Chini, L., Sahajpal, R., Froking, S., Bodirsky, B.L., Calvin, K., Doelman, J.C., Fisk, J., Fujimori, S., Klein Goldewijk, K., Hasegawa, T., Havlik, P., Heinemann, A., Humenöder, F., Jungclaus, J., Kaplan, J.O., Kennedy, J., Krisztin, T., Lawrence, D., Lawrence, P., Ma, L., Mertz, O., Pongratz, J., Popp, A., Poulter, B., Riahi, K., Shevliakova, E., Stehfest, E., Thornton, P., Tubiello, F.N., van Vuuren, D.P., Zhang, X., 2020. Harmonization of global land use change and management for the period 850–2100 (LUH2) for CMIP6. *Geoscientific Model Development* 13, 5425–5464. <https://doi.org/10.5194/gmd-13-5425-2020>.
- Jakimow, B., Griffiths, P., van der Linden, S., Hostert, P., 2018. Mapping pasture management in the Brazilian Amazon from dense Landsat time series. *Remote Sensing of Environment* 205, 453–468. <https://doi.org/10.1016/j.rse.2017.10.009>.
- 705 Jakovac, C.C., Dutrieux, L.P., Siti, L., Peña-Claros, M., Bongers, F., 2017. Spatial and temporal dynamics of shifting cultivation in the middle-Amazonas river: Expansion and intensification. *PLOS ONE* 12, e0181092. <https://doi.org/10.1371/journal.pone.0181092>.
- Janssen, T.A.J., Veraverbeke, S., 2025. What Are the Limits to the Growth of Boreal Fires? *Global Change Biology* 31, e70130. <https://doi.org/10.1111/gcb.70130>.
- 710 Jones, B., O'Neill, B.C., 2016. Spatially explicit global population scenarios consistent with the Shared Socio-economic Pathways. *Environ. Res. Lett.* 11, 084003. <https://doi.org/10.1088/1748-9326/11/8/084003>.
- Jones, C., Lowe, J., Liddicoat, S., Betts, R., 2009. Committed terrestrial ecosystem changes due to climate change. *Nature Geosci* 2, 484–487. <https://doi.org/10.1038/ngeo555>.
- Jones, M.W., Abatzoglou, J.T., Veraverbeke, S., Andela, N., Lasslop, G., Forkel, M., Smith, A.J.P., Burton, C., Betts, R.A., 715 van der Werf, G.R., Sitch, S., Canadell, J.G., Santín, C., Kolden, C., Doerr, S.H., Le Quéré, C., 2022. Global and Regional Trends and Drivers of Fire Under Climate Change. *Reviews of Geophysics* 60, e2020RG000726. <https://doi.org/10.1029/2020RG000726>.
- Jones, M.W., Veraverbeke, S., Andela, N., Doerr, S.H., Kolden, C., Mataveli, G., Pettinari, M.L., Le Quéré, C., Rosan, T.M., van der Werf, G.R., van Wees, D., Abatzoglou, J.T., 2024. Global rise in forest fire emissions linked to climate change in the 720 extratropics. *Science* 386, ead15889. <https://doi.org/10.1126/science.ad15889>.
- Kasoar, M., Perkins, O., Millington, J.D.A., Mistry, J., Smith, C., 2024. Model fires, not ignitions: Capturing the human dimension of global fire regimes. *Cell Reports Sustainability* 1, 100128. <https://doi.org/10.1016/j.crsus.2024.100128>.
- Keeley, J.E., Pausas, J.G., 2022. Evolutionary Ecology of Fire. *Annual Review of Ecology, Evolution, and Systematics* 53, 203–225. <https://doi.org/10.1146/annurev-ecolsys-102320-095612>.



- 725 Kirchmeier-Young, M.C., Malinina, E., Barber, Q.E., Garcia Perdomo, K., Curasi, S.R., Liang, Y., Jain, P., Gillett, N.P.,
Parisien, M.-A., Cannon, A.J., Lima, A.R., Arora, V.K., Boulanger, Y., Melton, J.R., Van Vliet, L., Zhang, X., 2024. Human
driven climate change increased the likelihood of the 2023 record area burned in Canada. *npj Clim Atmos Sci* 7, 316.
<https://doi.org/10.1038/s41612-024-00841-9>.
- Knorr, W., Kaminski, T., Arneth, A., Weber, U., 2014. Impact of human population density on fire frequency at the global
730 scale. *Biogeosciences* 11, 1085–1102. <https://doi.org/10.5194/bg-11-1085-2014>.
- Kreider, M.R., Higuera, P.E., Parks, S.A., Rice, W.L., White, N., Larson, A.J., 2024a. Fire suppression makes wildfires more
severe and accentuates impacts of climate change and fuel accumulation. *Nat Commun* 15, 2412.
<https://doi.org/10.1038/s41467-024-46702-0>.
- Kreider, M.R., Higuera, P.E., Parks, S.A., Rice, W.L., White, N., Larson, A.J., 2024b. Fire suppression makes wildfires
735 more severe and accentuates impacts of climate change and fuel accumulation. *Nat Commun* 15, 2412.
<https://doi.org/10.1038/s41467-024-46702-0>.
- Lampe, S., Gudmundsson, L., Kraft, B., Saux, B.L., Hantson, S., Kelley, D., Humphrey, V., Chuvieco, E., Thiery, W., 2025.
Modelling global burned area with deep learning (No. EGU25-15236). Presented at the EGU25, Copernicus Meetings.
<https://doi.org/10.5194/egusphere-egu25-15236>.
- 740 Lange, S., 2019. Trend-preserving bias adjustment and statistical downscaling with ISIMIP3BASD (v1.0). *Geoscientific
Model Development* 12, 3055–3070. <https://doi.org/10.5194/gmd-12-3055-2019>.
- Laris, P., 2002. Burning the Seasonal Mosaic: Preventative Burning Strategies in the Wooded Savanna of Southern Mali.
Human Ecology 30, 155–186. <https://doi.org/10.1023/A:1015685529180>.
- Li, S., Baijnath-Rodino, J.A., York, R.A., Quinn-Davidson, L.N., Banerjee, T., 2025. Temporal and spatial pattern analysis
745 of escaped prescribed fires in California from 1991 to 2020. *Fire Ecology* 21, 3. <https://doi.org/10.1186/s42408-024-00342-3>.
- Li, W., MacBean, N., Ciais, P., Defourny, P., Lamarche, C., Bontemps, S., Houghton, R.A., Peng, S., 2018. Gross and net
land cover changes in the main plant functional types derived from the annual ESA CCI land cover maps (1992–2015). *Earth
System Science Data* 10, 219–234. <https://doi.org/10.5194/essd-10-219-2018>.
- 750 Magnan, A.K., Schipper, E. I. f., Burkett, M., Bharwani, S., Burton, I., Eriksen, S., Gemenne, F., Schaar, J., Ziervogel, G.,
2016. Addressing the risk of maladaptation to climate change. *WIREs Climate Change* 7, 646–665.
<https://doi.org/10.1002/wcc.409>.
- Maia, P., Pausas, J.G., Vasques, A., Keizer, J.J., 2012. Fire severity as a key factor in post-fire regeneration of *Pinus pinaster*
(Ait.) in Central Portugal. *Annals of Forest Science* 69, 489–498. <https://doi.org/10.1007/s13595-012-0203-6>.
- 755 Malamud, B.D., Morein, G., Turcotte, D.L., 1998. Forest Fires: An Example of Self-Organized Critical Behavior. *Science*
281, 1840–1842. <https://doi.org/10.1126/science.281.5384.1840>.



- Mangeon, S., Voulgarakis, A., Gilham, R., Harper, A., Sitch, S., Folberth, G., 2016. INFERNO: a fire and emissions scheme for the UK Met Office's Unified Model. *Geoscientific Model Development* 9, 2685–2700. <https://doi.org/10.5194/gmd-9-2685-2016>.
- 760 Martens, B., Miralles, D.G., Lievens, H., van der Schalie, R., de Jeu, R.A.M., Fernández-Prieto, D., Beck, H.E., Dorigo, W.A., Verhoest, N.E.C., 2017. GLEAM v3: satellite-based land evaporation and root-zone soil moisture. *Geoscientific Model Development* 10, 1903–1925. <https://doi.org/10.5194/gmd-10-1903-2017>.
- Mathison, C., Burke, E., Hartley, A.J., Kelley, D.I., Burton, C., Robertson, E., Gedney, N., Williams, K., Wiltshire, A., Ellis, R.J., Sellar, A.A., Jones, C.D., 2023. Description and evaluation of the JULES-ES set-up for ISIMIP2b. *Geoscientific Model*
- 765 *Development* 16, 4249–4264. <https://doi.org/10.5194/gmd-16-4249-2023>.
- McClure, E.J., Coop, J.D., Guiterman, C.H., Margolis, E.Q., Parks, S.A., 2024. Contemporary fires are less frequent but more severe in dry conifer forests of the southwestern United States. *Commun Earth Environ* 5, 581. <https://doi.org/10.1038/s43247-024-01686-z>.
- Meijer, J.R., Huijbregts, M.A.J., Schotten, K.C.G.J., Schipper, A.M., 2018. Global patterns of current and future road
- 770 *infrastructure*. *Environ. Res. Lett.* 13, 064006. <https://doi.org/10.1088/1748-9326/aabd42>.
- Millington, J.D.A., Perkins, O., Smith, C., 2022. Human Fire Use and Management: A Global Database of Anthropogenic Fire Impacts for Modelling. *Fire* 5, 87. <https://doi.org/10.3390/fire5040087>.
- Moreira, F., Ascoli, D., Safford, H., Adams, M.A., Moreno, J.M., Pereira, J.M.C., Catry, F.X., Armesto, J., Bond, W., González, M.E., Curt, T., Koutsias, N., McCaw, L., Price, O., Pausas, J.G., Rigolot, E., Stephens, S., Tavsanoglu, C.,
- 775 *Vallejo, V.R., Van Wilgen, B.W., Xanthopoulos, G., Fernandes, P.M., 2020. Wildfire management in Mediterranean-type regions: paradigm change needed. Environ. Res. Lett.* 15, 011001. <https://doi.org/10.1088/1748-9326/ab541e>.
- Nikolakis, W., Roberts, E., 2020. Indigenous fire management: a conceptual model from literature. *Ecology and Society* 25. <https://doi.org/10.5751/ES-11945-250411>.
- Oliveras Menor, I., Prat-Guitart, N., Spadoni, G.L., Hsu, A., Fernandes, P.M., Puig-Gironès, R., Ascoli, D., Bilbao, B.A.,
- 780 *Bacciu, V., Brotons, L., Carmenta, R., de-Miguel, S., Gonçalves, L.G., Humphrey, G., Ibarregaray, V., Jones, M.W., Machado, M.S., Millán, A., de Morais Falleiro, R., Mouillot, F., Pinto, C., Pons, P., Regos, A., Senra de Oliveira, M., Harrison, S.P., Armenteras Pascual, D., 2025. Integrated fire management as an adaptation and mitigation strategy to altered fire regimes. Commun Earth Environ* 6, 202. <https://doi.org/10.1038/s43247-025-02165-9>.
- Parks, S.A., Guiterman, C.H., Margolis, E.Q., Lonergan, M., Whitman, E., Abatzoglou, J.T., Falk, D.A., Johnston, J.D.,
- 785 *Daniels, L.D., Lafon, C.W., Loehman, R.A., Kipfmüller, K.F., Naficy, C.E., Parisien, M.-A., Portier, J., Stambaugh, M.C., Williams, A.P., Wion, A.P., Yocom, L.L., 2025. A fire deficit persists across diverse North American forests despite recent increases in area burned. Nat Commun* 16, 1493. <https://doi.org/10.1038/s41467-025-56333-8>.
- Pelling, M., 2011. *Adaptation to Climate Change: From Resilience to Transformation*. Routledge & CRC Press. London & New York.



- 790 Perkins, O., Kasoar, M., Voulgarakis, A., Edwards, T., Haas, O., Millington, J.D.A., 2025a. The Spatial Distribution and Temporal Drivers of Changing Global Fire Regimes: A Coupled Socio-Ecological Modeling Approach. *Earth's Future* 13, e2024EF004770. <https://doi.org/10.1029/2024EF004770>.
- Perkins, O., Haas, O., Kasoar, M., Voulgarakis, A., Millington, J.D.A., 2025b. Supporting files for: Structural uncertainty in the direct human forcing of future global burned area. Zenodo. <https://doi.org/10.5281/zenodo.16635272>.
- 795 Perkins, O., Haas, O., Kasoar, M., Kelley, D., Teixeira, J.C.M., Voulgarakis, A., Millington, J.D.A., 2025c. Adapting to fire in a warming climate: towards global assessment of prescribed grazing and prescribed fire (No. EGU25-18640). Presented at the EGU25, Copernicus Meetings. <https://doi.org/10.5194/egusphere-egu25-18640>.
- Perkins, O., Kasoar, M., Voulgarakis, A., Smith, C., Mistry, J., Millington, J.D.A., 2024a. A global behavioural model of human fire use and management: WHAM! v1.0. *Geoscientific Model Development* 17, 3993–4016. <https://doi.org/10.5194/gmd-17-3993-2024>.
- 800 Perkins, O., Saxena, A., Seo, B., Millington, J.D.A., Brown, C., Rounsevell, M., 2024b. Gridded socio-economic capitals for the SSPs. Zenodo, <https://doi.org/10.5281/zenodo.14178581>.
- Perkins, O., Matej, S., Erb, K., Millington, J., 2022. Towards a global behavioural model of anthropogenic fire: The spatiotemporal distribution of land-fire systems. *Socio-Environmental Systems Modelling* 4, 18130–18130. <https://doi.org/10.18174/sesmo.18130>.
- 805 Rabin, S.S., Melton, J.R., Lasslop, G., Bachelet, D., Forrest, M., Hantson, S., Kaplan, J.O., Li, F., Mangeon, S., Ward, D.S., Yue, C., Arora, V.K., Hickler, T., Kloster, S., Knorr, W., Nieradzik, L., Spessa, A., Folberth, G.A., Sheehan, T., Voulgarakis, A., Kelley, D.I., Prentice, I.C., Sitch, S., Harrison, S., Arneth, A., 2017. The Fire Modeling Intercomparison Project (FireMIP), phase 1: experimental and analytical protocols with detailed model descriptions. *Geoscientific Model Development* 10, 1175–1197. <https://doi.org/10.5194/gmd-10-1175-2017>.
- 810 Randerson, J.T., Chen, Y., van der Werf, G.R., Rogers, B.M., Morton, D.C., 2012. Global burned area and biomass burning emissions from small fires. *Journal of Geophysical Research: Biogeosciences* 117. <https://doi.org/10.1029/2012JG002128>.
- Reichstein, M., Camps-Valls, G., Stevens, B., Jung, M., Denzler, J., Carvalhais, N., Prabhat, 2019. Deep learning and process understanding for data-driven Earth system science. *Nature* 566, 195–204. [https://doi.org/10.1038/s41586-019-0912-](https://doi.org/10.1038/s41586-019-0912-1)
- 815 1.
- Rosan, T.M., Sitch, S., Mercado, L.M., Heinrich, V., Friedlingstein, P., Aragão, L.E.O.C., 2022. Fragmentation-Driven Divergent Trends in Burned Area in Amazonia and Cerrado. *Front. For. Glob. Change* 5. <https://doi.org/10.3389/ffgc.2022.801408>.
- Russell-Smith, J., Yates, C.P., Edwards, A.C., Whitehead, P.J., Murphy, B.P., Lawes, M.J., 2015. Deriving Multiple Benefits from Carbon Market-Based Savanna Fire Management: An Australian Example. *PLOS ONE* 10, e0143426. <https://doi.org/10.1371/journal.pone.0143426>.
- 820 Schneider, T., Leung, L.R., Wills, R.C.J., 2024. Opinion: Optimizing climate models with process knowledge, resolution, and artificial intelligence. *Atmospheric Chemistry and Physics* 24, 7041–7062. <https://doi.org/10.5194/acp-24-7041-2024>.



- Sellar, A.A., Walton, J., Jones, C.G., Wood, R., Abraham, N.L., Andrejczuk, M., Andrews, M.B., Andrews, T., Archibald,
825 A.T., de Mora, L., Dyson, H., Elkington, M., Ellis, R., Florek, P., Good, P., Gohar, L., Haddad, S., Hardiman, S.C., Hogan,
E., Iwi, A., Jones, C.D., Johnson, B., Kelley, D.I., Kettleborough, J., Knight, J.R., Köhler, M.O., Kuhlbrodt, T., Liddicoat,
S., Linova-Pavlova, I., Mizielinski, M.S., Morgenstern, O., Mulcahy, J., Neininger, E., O'Connor, F.M., Petrie, R., Ridley,
J., Rioual, J.-C., Roberts, M., Robertson, E., Rumbold, S., Seddon, J., Shepherd, H., Shim, S., Stephens, A., Teixeira, J.C.,
Tang, Y., Williams, J., Wiltshire, A., Griffiths, P.T., 2020. Implementation of U.K. Earth System Models for CMIP6. *Journal*
830 *of Advances in Modeling Earth Systems* 12, e2019MS001946. <https://doi.org/10.1029/2019MS001946>.
Smith, C., Perkins, O., Mistry, J., 2022. Global decline in subsistence-oriented and smallholder fire use. *Nat Sustain* 5, 542–
551. <https://doi.org/10.1038/s41893-022-00867-y>.
Son, R., Ma, P.-L., Wang, H., Rasch, P.J., Wang, S.-Y. (Simon), Kim, H., Jeong, J.-H., Lim, K.-S.S., Yoon, J.-H., 2022.
Deep Learning Provides Substantial Improvements to County-Level Fire Weather Forecasting Over the Western United
835 States. *Journal of Advances in Modeling Earth Systems* 14, e2022MS002995. <https://doi.org/10.1029/2022MS002995>.
Son, R., Stacke, T., Gayler, V., Nabel, J.E.M.S., Schnur, R., Alonso, L., Requena-Mesa, C., Winkler, A.J., Hantson, S.,
Zachle, S., Weber, U., Carvalhais, N., 2024. Integration of a Deep-Learning-Based Fire Model Into a Global Land Surface
Model. *Journal of Advances in Modeling Earth Systems* 16, e2023MS003710. <https://doi.org/10.1029/2023MS003710>.
Stocker, B.D., Wang, H., Smith, N.G., Harrison, S.P., Keenan, T.F., Sandoval, D., Davis, T., Prentice, I.C., 2020. P-model
840 v1.0: an optimality-based light use efficiency model for simulating ecosystem gross primary production. *Geoscientific*
Model Development 13, 1545–1581. <https://doi.org/10.5194/gmd-13-1545-2020>.
Teckentrup, L., Harrison, S.P., Hantson, S., Heil, A., Melton, J.R., Forrest, M., Li, F., Yue, C., Arneth, A., Hickler, T., Sitch,
S., Lasslop, G., 2019. Response of simulated burned area to historical changes in environmental and anthropogenic factors: a
comparison of seven fire models. *Biogeosciences* 16, 3883–3910. <https://doi.org/10.5194/bg-16-3883-2019>.
845 van Vuuren, D.P., Edmonds, J., Kainuma, M., Riahi, K., Thomson, A., Hibbard, K., Hurtt, G.C., Kram, T., Krey, V.,
Lamarque, J.-F., Masui, T., Meinshausen, M., Nakicenovic, N., Smith, S.J., Rose, S.K., 2011. The representative
concentration pathways: an overview. *Climatic Change* 109, 5. <https://doi.org/10.1007/s10584-011-0148-z>.
Wang, H., Prentice, I.C., Keenan, T.F., Davis, T.W., Wright, I.J., Cornwell, W.K., Evans, B.J., Peng, C., 2017. Towards a
universal model for carbon dioxide uptake by plants. *Nature Plants* 3, 734–741. <https://doi.org/10.1038/s41477-017-0006-8>.
850 Wang, J., Sun, R., Zhang, H., Xiao, Z., Zhu, A., Wang, M., Yu, T., Xiang, K., 2021. New Global MuSyQ GPP/NPP Remote
Sensing Products From 1981 to 2018. *IEEE Journal of Selected Topics in Applied Earth Observations and Remote Sensing*
14, 5596–5612. <https://doi.org/10.1109/JSTARS.2021.3076075>.
Wi, S., Steinschneider, S., 2024. On the need for physical constraints in deep learning rainfall–runoff projections under
climate change: a sensitivity analysis to warming and shifts in potential evapotranspiration. *Hydrology and Earth System*
855 *Sciences* 28, 479–503. <https://doi.org/10.5194/hess-28-479-2024>.



Wooster, M.J., Roberts, G., Perry, G.L.W., Kaufman, Y.J., 2005. Retrieval of biomass combustion rates and totals from fire radiative power observations: FRP derivation and calibration relationships between biomass consumption and fire radiative energy release. *Journal of Geophysical Research: Atmospheres* 110. <https://doi.org/10.1029/2005JD006318>.